Diploma thesis

Charging of calcite(100) surface by contact with mineral particles studied by Kelvin Probe Force Microscopy

by

Stefan Klima

performed

at the Institute of Physics
Montanuniversität Leoben, Austria

under supervision of

Ao.Univ.-Prof. Dipl.-Phys. Dr.rer.nat. Christian Teichert
Dipl.-Ing. Dr.techn. Markus Kratzer
Mgr. inz. Monika Mirkowska

refereed by

Ao.Univ.-Prof. Dipl.-Phys. Dr.rer.nat. Christian Teichert

Leoben, June 2015

Eidesstattliche Erklärung

Ich erkläre an Eides statt, dass ich diese Arbeit selbstständig und ohne fremde Hilfe verfasst, andere als die angegebenen Quelle und Hilfsmittel nicht benutzt und mich auch sonst keiner unerlaubten Hilfsmittel bedient habe.

Affidavit

I declare in lieu of oath, that I wrote this thesis and performed the associated research myself, using only literature cited in this volume.

_____	_____
Datum	*Stefan Klima*

Abstract

Contact charging of mineral particles is an important topic within the framework of the industrially applied triboelectrostatic separation (TS) in mineral processing. During TS, charge is transferred between touching particles yielding positive/negative net charges on them. So far, the mechanism of charge transfer upon contact is still not well understood. In this work, the smallest subprocess which is the contact electrification upon contact with a single particle has been investigated in order to deepen insight into the charging behaviour. As a model system, the charging behaviour of a calcite(100) surface in contact with a single micrometer size mineral particle was investigated. For this purpose, a combination of atomic force microscopy (AFM) and Kelvin probe force microscopy (KPFM) was employed. An AFM based technique to rub a single, few 10 µm large particle with defined force and speed on a surface was developed.

The rubbing experiments with a particle glued to an AFM cantilever were done at two contact forces and at three different temperatures. After rubbing, the charging was monitored by measuring the local contact potential difference (CPD) using KPFM. Additionally, AFM force distance (FD) curves were recorded in order to quantify the occurring electrostatic forces. The surface analysis was performed using a standard conductive AFM tip. The analysed area (50 x 50 μm^2) was significantly larger than the rubbed area (20 x 20 μm^2). This allowed also observing possible long range influences on the surrounding area.

The change of the CPD depends on the rubbing material. Rubbing with a calcite particle leads to a decrease of the CPD, whereas rubbing with a quartz particle increases the CPD of the calcite(100) surface. An analysis of the temporal evolution of the CPD indicated an exponential decay of the introduced charge. FD curves revealed maximum electrostatic forces of ~45 pN, acting between AFM probe and charged areas. All of the conducted experiments demonstrate the applicability of the developed technique to study surface charging due to rubbing in triboelectrostatic separation.

Kurzfassung

Kontaktaufladung ist ein wichtiger Prozess im Rahmen der industriell eingesetzten Triboelektrostatischen Separation (TS) in der Mineralaufbereitung. Bei der TS kommt es während des Kontaktes zwischen zwei Partikeln zu einem Ladungsübertrag, welcher eine jeweilige positive oder negative Oberflächennettoladung erzeugt. Dieser Aufladungsprozess ist grundsätzlich bekannt, wird allerdings noch nicht im Detail verstanden. Im Rahmen dieser Diplomarbeit wird der kleinste Teilprozess, die Kontaktelektrifizierung durch ein einzelnes Partikel, untersucht. Als Modellsystem wurde das Aufladeverhalten einer Kalzit(100) Oberfläche durch Kontakt mit einem mineralischen Partikel untersucht. Für diese Untersuchung kam eine Kombination der Rastersondenmikroskopie (AFM) und der Kelvinsondenrasterkraftmikroskopie (KPFM) zum Einsatz. Es wurde eine auf AFM basierende Technik entwickelt, mit der es möglich ist, mit einem einzelnen, wenige 10 µm großen, mineralischen Partikel mit definierter Kraft und Geschwindigkeit auf einer Oberfläche zu reiben.

Die Experimente mit einem, auf einen AFM-Cantilever geklebten, Partikel wurden mit zwei unterschiedlichen Kräften sowie bei drei unterschiedlichen Temperaturen durchgeführt. Die Aufladung wurde durch Messen der lokalen Kontakt-Potential-Differenz (CPD) mittels KPFM aufgezeichnet. Die Oberflächenanalyse geschah mit einer leitfähigen AFM Spitze. Außerdem wurden mit dieser Kraft Abstandskurven aufgenommen, um die auftretenden elektrostatischen Kräfte quantifizieren zu können. Die analysierte Fläche (50 x 50 μm^2) war signifikant größer als die geriebene Fläche (20 x 20 μm^2). Dies erlaubt, den möglichen Einfluss des Reibens auf den, die geriebene Fläche umgebenden Bereich zu untersuchen.

Die Änderung des CPD-Signals hängt vom Material des reibenden Partikels ab. Reiben mit Kalzit führt zu einer Abnahme der CPD, wohingegen Reiben mit Quartz die CPD der Kalzit(100)-Oberfläche erhöht. Des Weiteren wurde eine exponentielle Abnahme der eingebrachten Ladung mit der Zeit festgestellt, welche sich gut über die gemessene CPD verfolgen lässt. Eine Analyse der Kraft Abstandskurven ergab maximal auftretende elektrostatische Kräfte von ~45 pN zwischen der AFM Sonde und den am stärksten geladenen Flächen. Alle durchgeführten Experimente zeigen die Anwendbarkeit von der dafür entwickelten Technik, um die Aufladungen infolge des Reibprozesses in der Triboelektrostatischen Separation zu untersuchen.

Acronyms

AFM	Atomic Force Microscopy
CM	Contact mode
NCM	Non-contact mode
TM	Tapping mode
KPFM	Kelvin Probe Force Microscopy
SEM	Scanning Electron Microscopy
FD	Force-Distance
FM	Force Map
CPD	Contact Potential Difference
RMS	Root mean square
TS	Triboelectric Separation
SP	Surface Potential
UV-light	Ultra violet light
AR	Asylum Research

Index of Contents

1 Motivation

Triboelectrostatic Separation is used in mineral processing for the production of powders of high purity [28]. High purity powders are important for many different technical applications. They are used in the building materials industry, chemical industry or as filler medium in plastics, colours or papers.

Triboelectrostatic separation is based on the triboelectric effect. Triboelectricity concerns the charge transfer between objects that are brought into mechanical contact and the net charge resting on them after separation. Crucial for the charging is mainly the contact between the two objects. Even particles of the same material might carry a net charge after contact. The charge transfer is strongly determined by the difference in their work function, which depends on the specific surface conditions. When two particles are in contact, in general a charge flow occurs from one surface to the other [33]. This charging process is influenced by a number of different parameters. It depends on the material, contact area, time, force, environment conditions, and the possible existence of a fluid (water) film on the surface [13,15,16]. Even though TS has been successfully applied to separate the fractions from mineral powder mixtures, details of the charging process are vastly unknown.

Investigations on the charge exchange between a mineral particle rubbed against a $CaCO_3$(100) surface, are carried out in the SPM Group at the Institute of Physics (Montan-universität Leoben). Atomic force microscopy (AFM) and Kelvin probe force microscopy (KPFM) methods are used to characterize surface properties and charge transfer [3].

One topic of this thesis is the development of a method to rub a few 10 µm-size mineral particle with defined force and speed on a mineral surface. The measurements were performed in an AFM from Asylum Research (AR). The necessary requirements for such experiments were done by gluing the mineral particle onto the end of an AFM-cantilever. The quality and usability of the modified cantilevers were checked with SEM [30].

The second topic focuses on the charging of the $CaCO_3$(100) surface by rubbing with two different types of mineral particles (calcite and quartz). The rubbing results were analysed as a function of material, rubbing force, and temperature. The main question was whether charging, the visualization, and measurability of the accumulated charge on the mineral surface is possible.

2 Methodology

2.1 Materials

For the investigation of the triboelectric charge on a $CaCO_3$(100) surface, two different minerals were chosen as rubbing materials. The first is calcite itself, the other is quartz. Both minerals are often components of the same raw material and also of the mineral powder before separation. It is useful to compare those two minerals because they are both purified via the same TS process.

Calcite

Calcite is a mineral containing Calcium (Ca) and Carbon trioxide (CO_3) in a ratio of 1:1, $CaCO_3$. The hardness of minerals is classified with the Mohs scale. Here, the mineral hardness is compared with the hardness of 10 reference minerals (10 diamond, 1 talc). In the Mohs hardness scale calcite is classified in category 3. This means that calcite is a quite soft material [6].

Quartz

In comparison to calcite is quartz (SiO_2) a very hard crystalline mineral (Moh's hardness: 7) with a trigonal unit cell. The hardness of quartz is much higher than that of calcite. This is important for the rubbing process during the measurements, because rubbing with a hard particle on a soft $CaCO_3$(100) surface can cause surface wear [32].

Table 2.1: Properties of the used mineral powders [25].

Particle material	Commercial name	Source	Preparation method	Particle size [µm]
$CaCO_3$ (calcite)	Marble A	From natural deposit	Pick up by hand, crush mechanical without chemical additives	5 - 50
SiO_2 (quartz)	Microsil M6		Milled, dried, classified, controlled additive amount, hand-sieved (between sieves with meshes 270 and 500)	25 - 53

2.2 Atomic Force Microscopy

Atomic force microscopy (AFM) based methods are high-resolution techniques using a sharp tip for imaging. The theoretical resolution limit is determined on the tip radius, even atomic resolution is possible. The imaging concept is quite different to that of an optical microscope. A sharp tip attached to the end of a cantilever (usually made of silicon) is scanned across a surface. In the original concept the image is generated by recording the deflection of the cantilever caused by tip-sample interaction [21]. Piezoelectric actuators are responsible for the movement of the tip in x-, y-, and z-direction. The detection of the cantilever deflection is realized with an optical system consisting of a laser and a four-segment position sensitive photodiode. The back side of the cantilever is often metal coated to increase reflectivity. The laser beam is reflected from the back side of the cantilever to the four-segment photodiode. If the tip moves across the surface the cantilever deflects and the laser spot on the photodiode also moves. The moving laser spot generates different electrical signals on the four segments of the photodiode (Figure 2.1). These signals are digitally processed and converted into an image of the surface [8,20,29].

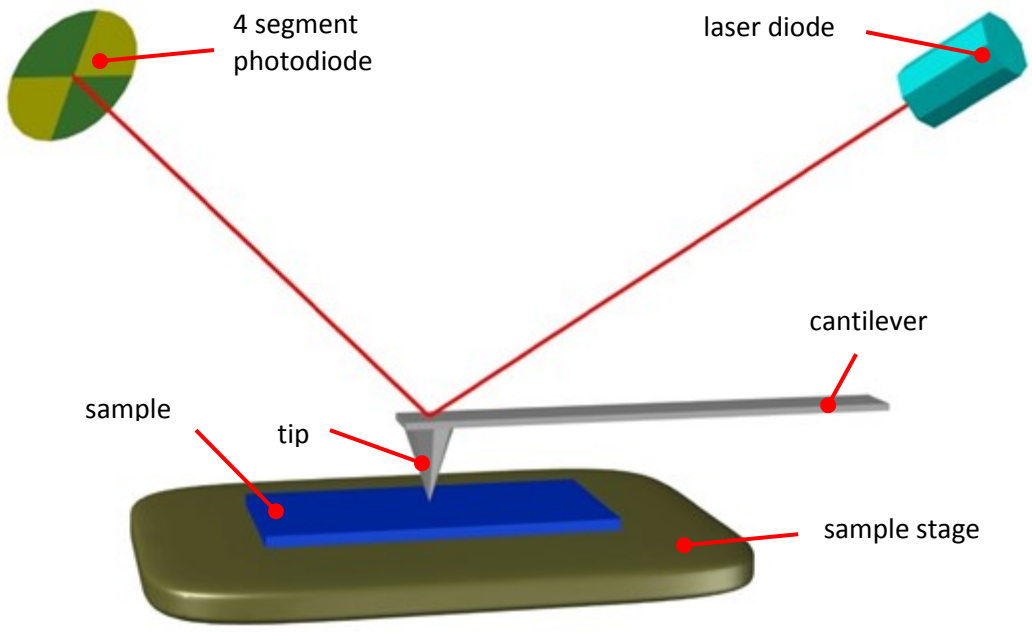

Figure 2.1: Schema of an AFM.

For image recording, different techniques have been developed. Basically three standard modes can be used for topography imaging: contact, non-contact and tapping mode (intermittent contact mode).

Contact mode (CM) [8,29]

In contact mode, the tip stays permanently in contact with the sample surface while the cantilever is scanned across the surface. Contact mode can be further divided into two different operational principles (Figure 2.2), the constant height and the constant force mode.

In constant height mode, the level of the cantilever above the surface is held constant with respect to the initial point of the measurement, so there is no need of a feedback system. Differences in surface height bend the cantilever more or less causing a change in the deflection signal which can be converted into topographic information (Figure 2.2a).

The constant force mode (Figure 2.2b) has more complex requirements than the constant height mode. In this case, a feedback is active adjusting the z-piezo position such that the cantilever deflection is kept constant. The recorded movement of the z-piezo as function of the lateral position yields a topographic map.

The permanent contact between tip and surface during scanning can lead to some problems. On soft surfaces the tip might scratch over the surface and redistribute material to the rims of the scanned area. Additionally, shear forces can distort the measured surface characteristics. Another problem of the permanent contact is the influence on the tip itself. It can pick up particles or the tip can easily be damaged during the scanning. In the worst case the tip can be destroyed. This is predominantly a problem of the constant height mode.

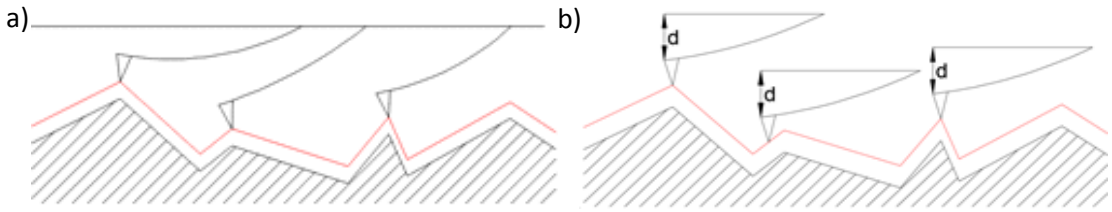

Figure 2.2: Working principle of: a) constant height mode and b) constant force mode.

Dynamic modes

Non-contact mode [8,29]

In order to avoid damage of tip or sample dynamic modes have been developed. In non-contact mode, the tip is never in the repulsive interaction with the sample surface. The cantilever is excited to oscillate at its resonant frequency. In non-contact mode the oscillation amplitude is typically <10 nm. When the tip comes near the surface, long range forces like Van der Waals or electrostatic forces decrease the resonance frequency of the cantilever. This decrease in frequency is compensated by a feedback loop system by

adjusting the tip surface distance. In this way a topographical image is generated. In non-contact mode, the cantilever oscillates a few nanometers above the surface and the tip is only weakly interacting. Therefore non-contact mode is favoured in high or ultra-high vacuum systems. It is also the most used method for very soft and biological materials.

The problem of the dynamic mode is the speed of this method. It is slower than the other AFM scanning modes.

Tapping mode (TM) [8, 29]

The difference to non-contact mode is the working point of the oscillation stimulation of the cantilever. Tapping mode works near and not at the resonance frequency at significantly higher oscillation amplitudes. For tapping mode, the amplitude is usually about 200 nm.

There are two different possibilities acquiring an image in tapping mode. The first measures changes in the resonance frequency (frequency modulation), similar to non-contact mode. The second possibility relies on the changes in amplitude (amplitude modulation) due to the interaction, between tip and surface. While non-contact mode is used under high and ultra-high vacuum conditions, tapping mode is typically used under ambient conditions. Since the tip is just for a very short time during one oscillation in “contact” to the surface, lateral forces are practically negligible. Therefore, tip and surface wear are drastically reduced. Thus, even very fine tips, necessary for high resolution, last very long and proper imaging is possible. However, tapping mode is susceptible for scanning artefact related to different possible tip-surface interactions regimes. Especially a compositional inhomogeneous surface the tip-surface interaction can jump between repulsive and attractive, which can lead to incorrect height data.

2.3 Kelvin Probe Force Microscopy

Measurement principle

The Kelvin probe force microscopy (KPFM) is an AFM based imaging technique to visualize and quantify the contact potential difference (CPD) between the sample surface and the tip. For KPFM, a conductive AFM tip is needed. The tip and the surface form a capacitor sensitive to electrostatic interactions. The principle of KPFM is illustrated in Figure 2.3.

A plate capacitor is used as model to describe the KPFM measurement. The conductive tip and the sample surface have different work functions. In this system, the conductive tip is the electrode with known work function. If the tip and the surface come close, electrons flow from the lower work function material to the electrode with higher work function

causing a potential difference. This is called the contact potential difference. The CPD causes electrostatic forces between the surface and AFM probe. These forces can be compensated by applying a DC voltage to the probe (or sample). The forces cancel out when the value of the DC tip bias matches the CPD. Technically the detection is carried out by applying the sum of an AC and a DC voltage to the tip. The cantilever oscillations at the frequency ω of the AC voltage are measured with a lock–in technique. The feedback adjusts the V_{DC} to nullify the oscillation at ω (which is caused by the electrostatic forces) at every point of the surface ($V_{tip} = V_{DC} + V_{AC}\sin(\omega t)$) [3]. The KPFM measurement uses a two pass mode. In the first scan line the topography is determined. In the second pass of the same scan line, the tip is lifted up for several nm and the ac bias is applied. This allows to avoid topographical influences during the detection of the electrostatic forces by KPFM [1,21,22]. The working scheme is presented in Figure 2.3.

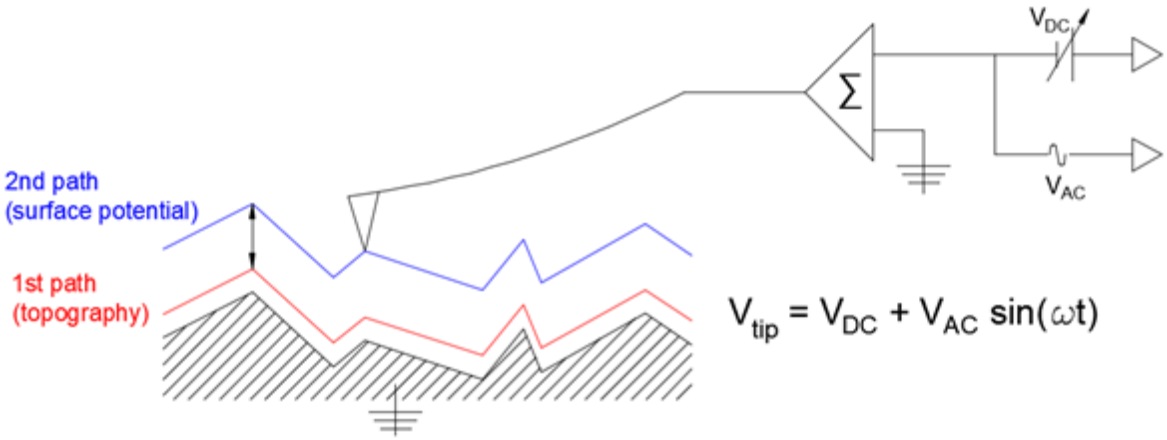

Figure 2.3: Two pass measurement technique of KPFM.

Analysis of AFM and KPFM images

The recorded AFM and KPFM images were analysed with the freeware program Gwyddion. Force distance curves were analysed with Origin 9.1 [9].

2.4 Force Distance Curve

A force distance (FD) curve is a simple and fast possibility for mechanical surface analysis. It records the forces acting on the cantilever when the tip approaches, indents in and retracts from the surface. This technique shows attractive or repulsive forces between tip and sample surface, as well as plastic and elastic deformations [4,17].

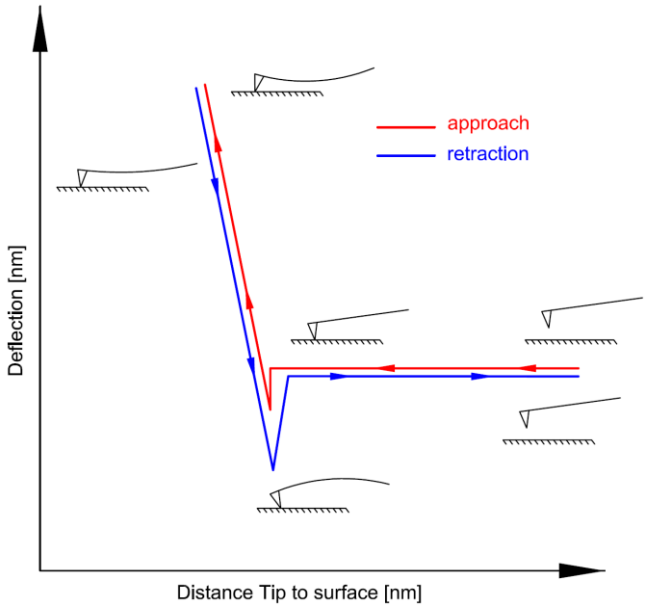

Figure 2.4: Typical approach and retraction of a cantilever during a force distance curve.

The working principle of a FD curve is illustrated in Figure 2.4.

- The tip starts at a defined distance above the surface (few µm away). The deflection of the cantilever is net attractive (bending to the surface) or repulsive (bending away from the surface).
- In contact, the repulsive forces bend the cantilever towards.
- After a pre-defined set point of deflection is reached, the movement is reversed and the deflection decreases again.
- Due to attractive forces, the cantilever bends upwards the surface (tip sticks to the surface).
- An interesting point is the deepest deflection value of the reversed movement. It yields the magnitude of the adhesive force between surface and tip. The lower the deflection value before losing contact the higher is the adhesive force between tip and surface.
- After the jump out of contact, the cantilever again moves away from the surface.

2.5 Force Map

A force distance curve yields information about one specific place on the surface. When more information is needed, an array of force distance curves has to be measured. A set of them measured in a raster provides information of a larger surface area. This measurement method is called force map [34]. There are three main parameters which can be adjusted: number of points, strength of the indentations, and measurement speed.

For the measurements in this thesis, a raster of 32 x 32 points is used. In Figure 2.5 the single indentation points can be seen well. Each contact between tip and surface influences the surface potential. So each contact during the measurement gives a little point like charge [3]. In Figure 2.5, these point charges are well distinguishable from the background. The background arises from the contribution of all adjacent points to the measured potential. Further, a spreading of changes away from the contact points might also contribute.

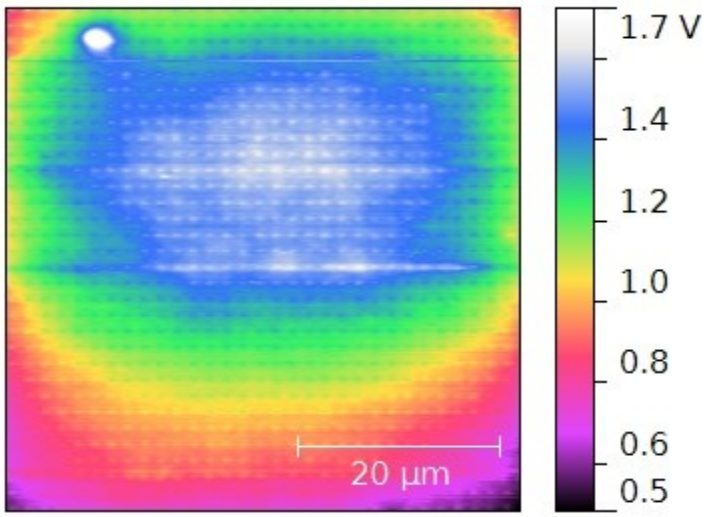

Figure 2.5: KPFM image of the $CaCO_3$(100) surface (rubbing with calcite at 0.1 µN and 50 °C) after the first force map sequence, before rubbing. Every single contact point of each FD curve is visible.

3 Experimental

3.1 Surface material

The investigated mineral surface is a calcite single crystal in (100) orientation. This single crystal plate has the dimensions of 10 x 10 x 0.5 mm^3 [26]. For the electrical grounding, the calcite plate was glued to an AFM metal specimen disk with silver paste. This metal disk consists of stainless steel (alloy 430) and has a diameter of 12 mm and a thickness of 0.76 mm [27].

3.2 AFM Probes

The measurements of this thesis were performed with NSG30/TiN probes from the company NT-MDT. These are tapping mode probes with a silicon cantilever and a TiN conductive coating. The complete probe specifications are listed in Table 1.

Table 3.1: NSG30/TiN specification [10].

Tip curvature radius	Cantilever length, L ± 5 µm	Cantilever width, W ± 5 µm	Cantilever thickness	Resonant frequency	Force constant
35 nm	125 µm	40 µm	4 µm	240-440 kHz	22-100 N/m

Rubbing a µm-size mineral particle against the $CaCO_3$(100) surface with defined force and speed is accomplished by using an AFM cantilever with a particle attached. Gluing a particle on a cantilever's ending is therefore a central task. For this, used NSG30/TiN probes were used, because a "good" tip is not necessary and makes handling easier, because of the same dimensions (cantilever change during the measurement sequence) of the modified cantilevers. The glued mineral particles consist of calcite or quartz having a particle size of around 30 µm. In Figure 3.1 scanning electron microscopy (SEM) images of modified cantilevers are presented.

For attaching a particle the glue Norland Optical Adhesive 68 [24] was used. This is a clear, colourless polymer glue, which cures under UV-light.

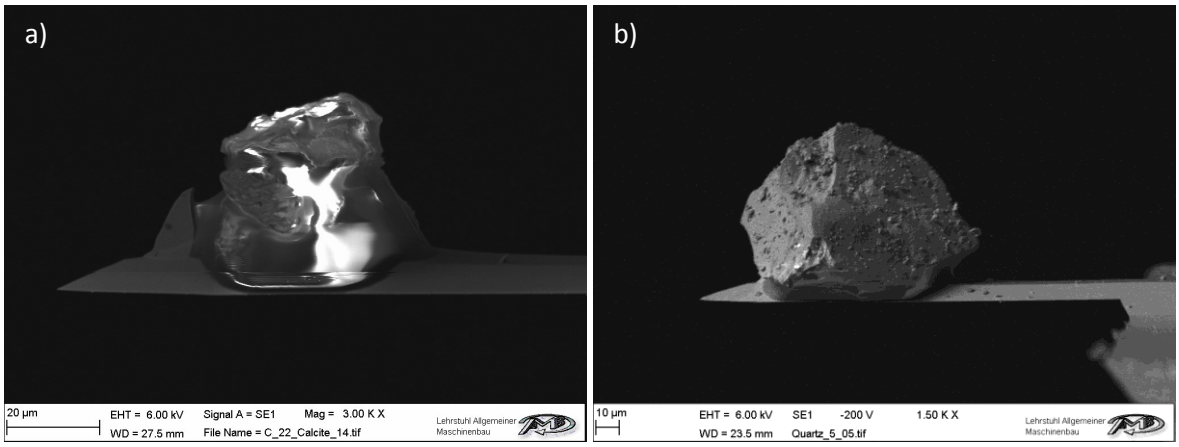

Figure 3.1: SEM image of: a) glued quartz and b) calcite particle.

3.3 Gluing a particle onto a tip

The preparation of the particle modified tip is a gluing process on the µm scale. Different methods are known to glue particles on an AFM cantilever [2]. The tip has to touch the glue to get covered with it to finally hold a mineral particle. The problem of this simple process is the small size of the objects. Covering a tip with a height of 14 to 16 µm with glue or picking up a particle with a size of 30 µm is not as simple. Therefore, the whole modification process was done directly in the AFM using it's built in optical microscope.

A standard cover glass was used as substrate for the mineral powder and the polymer glue (Norland Adhesive 68). Small amounts of calcite/quartz powder were dispersed on one side of the glass and on the other one a thin band of glue was spread. This is presented schematically in Figure 3.2.

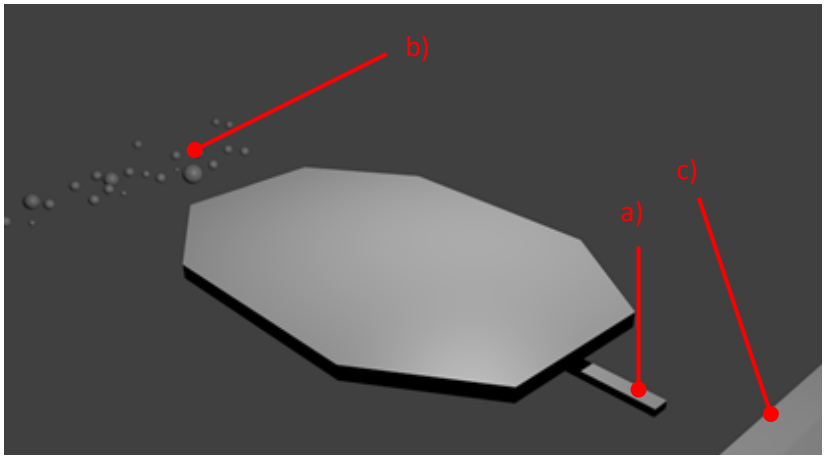

Figure 3.2: Starting position of the cantilever:
a) cantilever; b) Powder with different grain size; c) glue.

In a first step, the tip has to be covered with glue. This is illustrated in Figure 3.3. For this purpose, it is positioned on the cover glass above the glue band, because the tip has to be lowered carefully from the top into the glue. When approaching it too hasty, the whole cantilever might get sucked into the glue. The approach from the top is necessary to ensure that primarily the tip gets into contact with the glue and not the entire cantilever. The tip is only 14 to 16 µm high and the cantilever has a reflective coating on the upper side. When the penetration is too deep or happens at an unfavourable angle the whole cantilever gets covered with glue. In this case, the reflective top surface of the cantilever is covered by the glue and a proper response of the reflected laser beam on the deflection is obstructed. Another problem is that a too large amount of glue can have an effect on the particle selection process. The glue might cover the whole particle, preventing direct contact between mineral particle and mineral surface making investigations on mineral-mineral contact charging impossible.

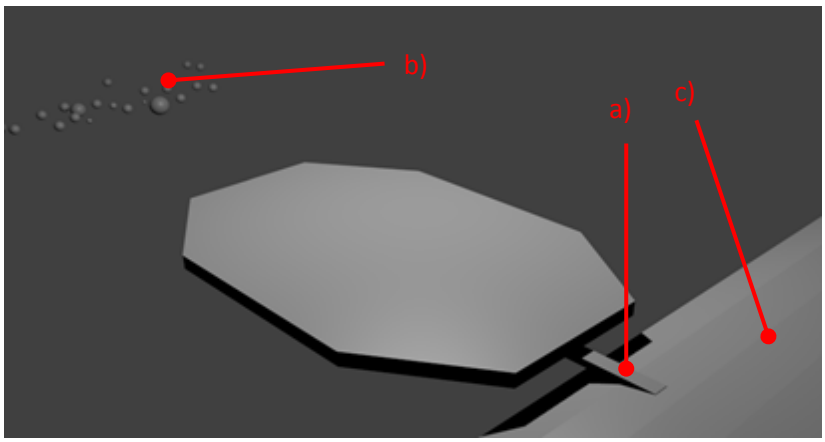

Figure 3.3: Lowering the AFM cantilever into the glue:
a) cantilever; b) powder with different grain size; c) glue band.

After covering the tip with the appropriate amount of glue, a particle with suitable size has to be found. This is presented in Figure 3.4. It is not possible to make an AFM height scan with a glue covered tip, so only the two-dimensional view from the optical microscope can be used for the selection process. These mineral particles under investigation are usually no spheres but faceted crystalline grains. There can be a large difference in height between two particles with the same lateral size. Here, the correct size is important for the rubbing process. The tip has a height of 14 to 16 µm, if the particle is smaller than the tip height, the rubbing most probably occurs with the tip and not with the particle. A too large particle is also a problem, because this leads to uncontrollable movements during the rubbing process. In the worst case the cantilever can break, because of the strong bending of the cantilever.

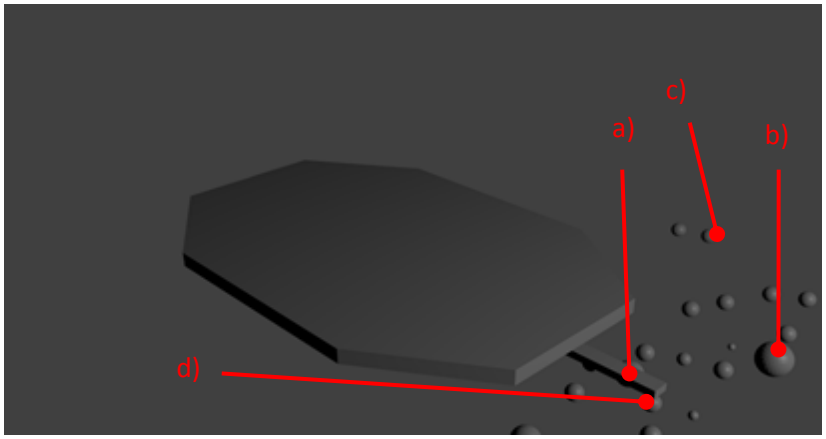

Figure 3.4: Attaching an appropriate particle to the glue covered AFM tip:
a) cantilever; b) large particle; c) small particle; d) particle with correct size.

After attaching the appropriate particle to the cantilever, the glue has to be hardened under UV-light for an hour. This is necessary, because the used polymer glue (Norland Optical Adhesive 68) only cures under UV-light (maximum absorption wavelength between 350-380 nm). Apparently, there are some criteria which have to be checked after the preparation process, because it is impossible to make a statement of the usability of the modified tip. For this, the following characterization of the modified tip is essential.

3.4 Characterization of the modified AFM probes

The usability of the modified probes has to be confirmed by checking the particle size and the amount and distribution of the glue. The characterization was done in a SEM (EVO MA15) [30]. Characterizing a cantilever needs time, therefore it is an advantage that it was at least possible to perform a preselection by determination of the cantilever resonance frequency in the AFM. If a particle is glued to the tip, the mass of the probe changes, which in turn changes the resonance frequency. A big change in resonance frequency indicates a big particle, whereas for a small change a small particle can be expected. Comparisons of the first SEM measurements with the corresponding resonance frequencies allowed specifying a certain range of resonance frequency changes indicative for a successful modification. A simple measurement of the resonance frequency directly after the gluing process was then sufficient to sort out cantilevers with bad preparation.

SEM was used for further characterization of the modified cantilevers. It allows the decision of the usability of the probe, because it is possible to differentiate between the tip, the cantilever, the glue and the mineral particle.

Good modified probes have the glue only on the bottom side of the particle, the top rubbing area is pure mineral. Another point of the usability of the modified probes is the size of the particle. It has to be larger than the tip, but not too large to influence the bending of the cantilever (twist or unusual bending).

Figure 3.5 shows two modified cantilevers with calcite particles with appropriate size. The amount of glue is on both cantilevers quite large, but does not cover the top of the particles. On the left SEM image (Figure 3.5a), the tip is visible. Here, it can be seen that the tip apex is deformed due to the measurement performed earlier (used probe). In the second example (Figure 3.5b) the tip is completely covered.

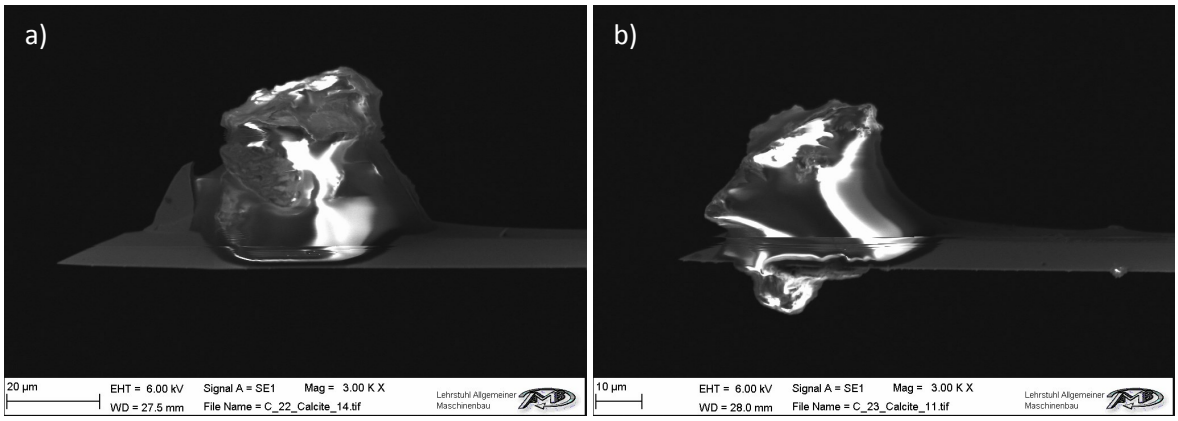

Figure 3.5: SEM micrographs of glued calcite particle with correct size on NSG30/TiN cantilever: a) particle with the correct amount of glue on the base; b) glue covers both side of the cantilever.

Two of the modified tips showed a big difference in resonance frequency. The very low frequency indicates that the particle is very large. Under the SEM this assumption could be confirmed. On the left image (Figure 3.6a) the particle is very large in comparison to the cantilever. The second picture (Figure 3.6b) shows a base of glue with a particle sitting on top.

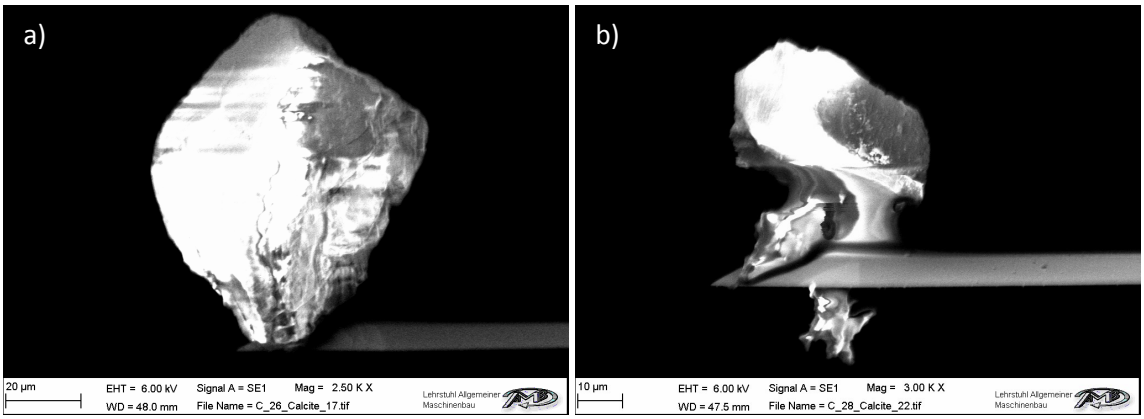

Figure 3.6: SEM images of very large glued calcite particle on NSG30/TiN cantilever: a) too large glued particle; b) glue base with uplifted particle.

The first five tip modifications with quartz particles failed. The grain size of the quartz powder was too fine. Therefore, not a single particle, but a conglomerate of the powder has been accumulated on the cantilever. Examples are presented in Figure 3.7.

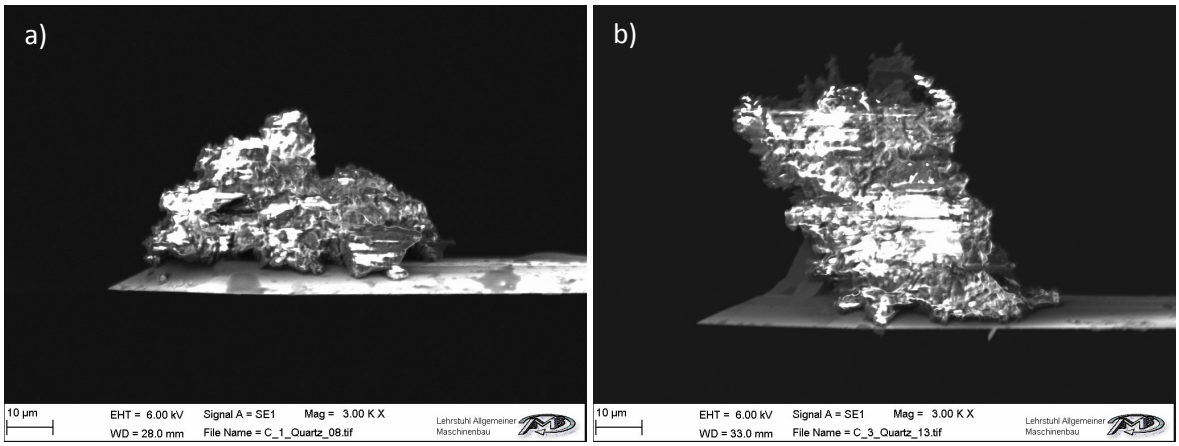

Figure 3.7: SEM images of glued quartz conglomerate on NSG30/TiN cantilever: a) conglomerate covers the tip; b) conglomerate lying on the tip.

The rather undefined structure of this conglomerate is problematic. The distribution of glue within the conglomerate is unknown. Further it is easily possible that the structure deforms resulting in an unstable contact during rubbing.

Therefore, a second quartz powder with coarse grains was tested and turned out to be more useful. The modified tips exhibit the correct grain size with small amounts of glue on the bottom side. The particles are quite large, but small enough for the measurements. In contrast to the calcite particles, the quartz grains often appear to be more irregular exhibiting rather sharp apexes as is shown in Figure 3.8.

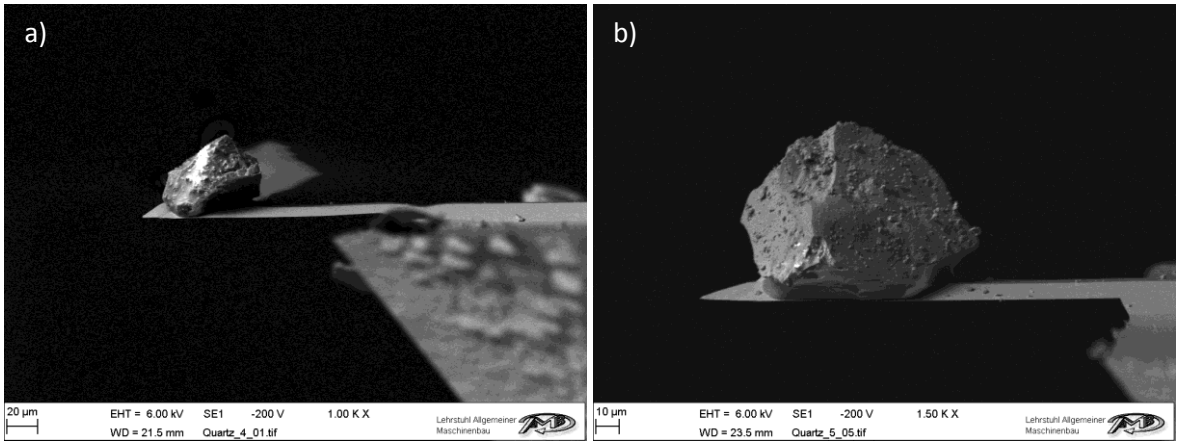

Figure 3.8: SEM micrographs of glued quartz particle from the 2nd quartz powder: a) particle with sharp apex on top; b) quite large particle with single apex.

3.5 Overall measurements procedure

The point of interest is the surface charging upon rubbing with a mineral particle on a calcite(100) surface. It is necessary to obtain information on the pristine surface to see the differences induced by the rubbing process. Every contact influences the charge states of the surface. Therefore, a measurement sequence has to be defined in order to obtain reproducible results.

A number of preliminary tests were performed to get an idea, how large the influence of the different approaches is and which sequence works most reliable. Figure 3.9 presents the selected sequence which consists of three measurement steps, which were repeated twice with a rubbing step in-between.

Before the measurement, the whole system was heated up to 130 °C for one hour to reduce the water and volatile contaminations from the surface. The sequence starts with a Topography/KPFM measurement. Step one is performed with an unmodified NSG30/TiN conductive probe. A 50 x 50 μm^2 AFM/KPFM scan turned out to be practical.

Force mapping is the second step within the surface analysis. Force distance curves with 32 x 32 points over the whole 50 x 50 μm^2 area are recorded. The higher the electrostatic interaction, the stronger is the deflection of the cantilever near the surface. These deflection values are visualized in a diagram, and so the FD curves before and after rubbing can be compared.

The third step is a repetition of the first. Here, the influence of the force map becomes visible. This third step is very important, because force mapping can influence the surface mechanically or electrically due to the fact that every FD curve represents an intimate touching between tip and surface.

The most interesting step in the whole measurement sequence is the fourth, which is the rubbing with the mineral particle on the $CaCO_3$(100) surface. One of the problems with this step is the necessity of a cantilever change, because the rubbing is done with the modified probe and the KPFM measurements with a standard NSG30/TiN. The biggest problem was to relocate the same position after the cantilever change (see chapter 3.6). The rubbing area was 20 x 20 μm^2 to obtain information of the rubbed region and from the surrounding of the rubbed area.

For the fifth step a further cantilever change was necessary. Then, the steps one to three were repeated to observe the changes in topography and CPD signal.

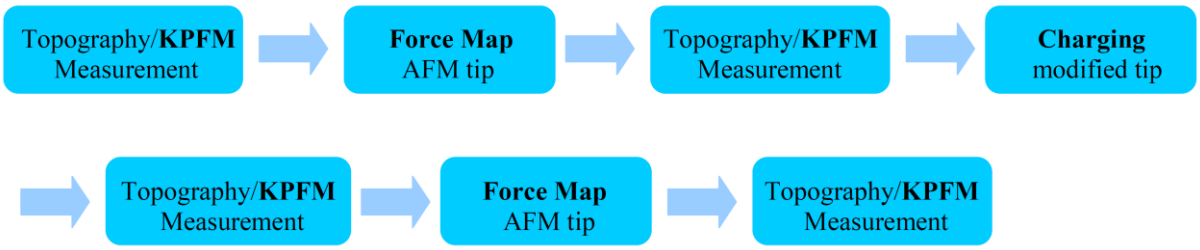

Figure 3.9: Schematic diagram of the experimental sequence of the alternating analysing and rubbing processes.

3.6 Positioning

A complete measurement sequence requires both types of probes. The standard NSG 30/TiN for KPFM and force mapping, and the modified one for the rubbing step. Therefore, it is necessary to change the cantilever between the measuring and rubbing processes. After changing the cantilever, a repositioning of the scanner has to be performed to find the original position on the sample surface. The scanning position has to be the same to compare the CPD signal before and after the rubbing process. The differences in scan size and positioning between analysing and rubbing sequence are presented in Figure 3.10.

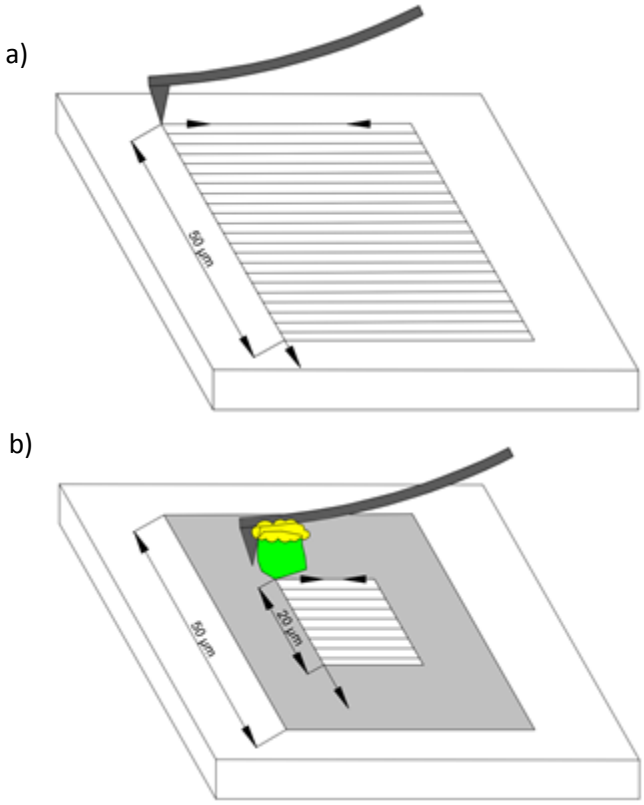

Figure 3.10: Scheme of rubbing with:
a) 50 x 50 µm^2 with the NSG30/TiN tip; b) 20 x 20 µm^2 with the modified tip.

The repositioning is not a single step problem between KPFM and rubbing. In order to find the same position every time again, it is necessary to start the measurement at a location which is easy to identify already in the optical microscope. Good orientation marks are occasional dust particles on the $CaCO_3$(100) surface. They often have unique shapes and making the recognition easier.

All scans were performed from top to bottom (fast scan axis from left to right and slow scan axis from top to bottom). A starting position 10 µm under a dust particle has proven to work well as is illustrated in Figure 3.11.

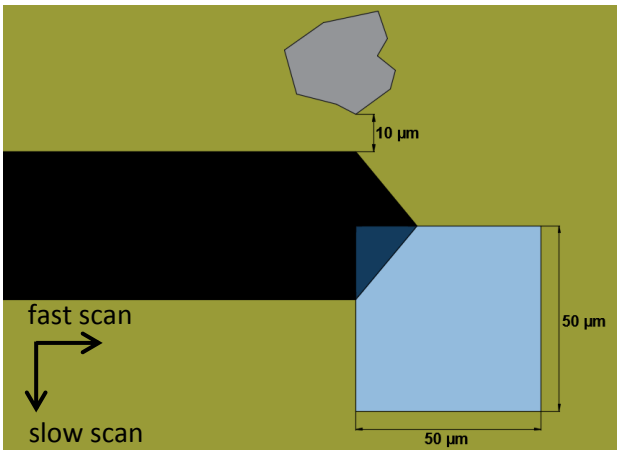

Figure 3.11: Positioning of the cantilever placed 10 µm below a landmark (dust particle) on the $CaCO_3$(100) surface. The scan area is indicated by the shaded square. The tip is assumed to be located in the upper left corner to the indicated scan area.

The exact position can be found by comparing the AFM height images before and after rubbing. Also in the height images, unique topography features can be found making a position control possible. Examples such features enabling a proper repositioning are presented in Figure 3.12 and Figure 3.13. In the height images for calcite rubbed on $CaCO_3$(100) specifically shaped and arranged dust particles are visible (marked by red circles) which can be used for orientation and proper cantilever positioning.

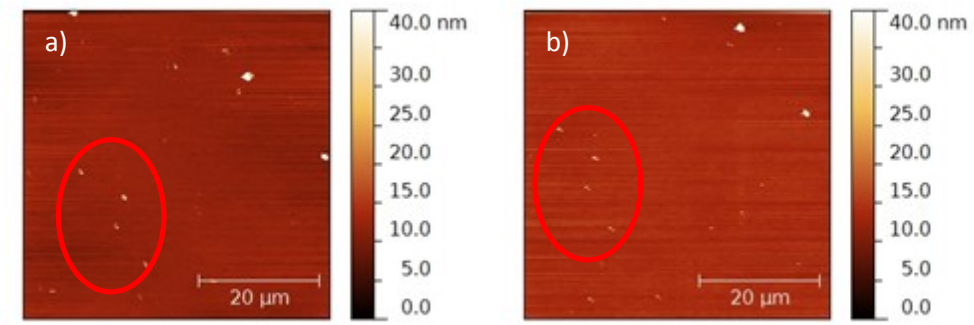

Figure 3.12: AFM height images with many dust particles on the left side: a) before rubbing/force mapping; b) after rubbing at 40 °C; 0.01 µN.

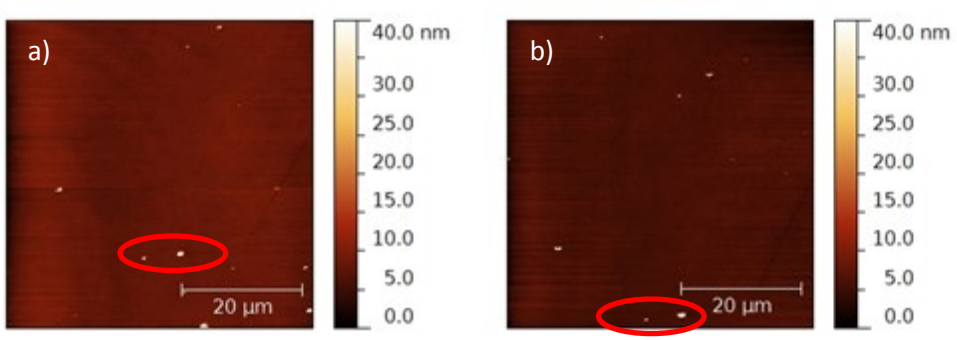

Figure 3.13: AFM height images with a pair of dust particles:
a) before rubbing/force mapping; b) after rubbing at 30 °C; 0.1 µN.

3.7 AFM System

All measurements were performed using an MFP 3D system from Asylum Research (AR) [18], presented in Figure 3.14. The AFM has a closed loop scanner, which monitors the actual movement and position of the piezoelectric actuators. For vibration damping, the AFM sits on an active vibration isolation system (Halcyonics Micro 40) [19].

For the investigation of the rubbing influence at different temperatures a heating stage (also AR) was used (described in chapter 3.8).The $CaCO_3$(100) crystal was fixed on a metal plate and placed in the heating stage.

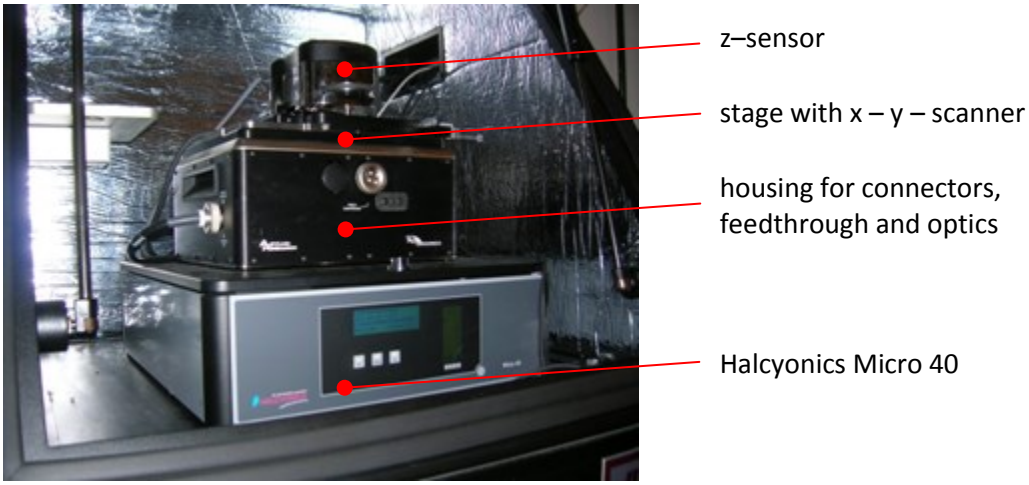

Figure 3.14: Photograph of an Asylum Research MFP-3D AFM [36].

3.8 Heating Stage

Figure 3.15 shows a scheme of the PolyHeaterDSHR (DSHR - Dry Sample Thermal Accessory) heating stage from Asylum Research. It allows to heat dry samples up to 300 °C. The temperature offset is less than 0.2 °C. The temperature controlled surface (Sample Mount) is magnetic and has a diameter of 12 mm, the maximum sample thickness is supported up to 2 mm. A metal clip (sample clip holder) is used for holding the sample down on the sample mount. In this diploma thesis, the Heater Stage (HS) was used to control the temperature during the measurement. Experiments were carried out at 30 °C, 40 °C, and 50 °C. It is also used to get rid of the water layer on the surface, for this the sample gets heated up to 130 °C.

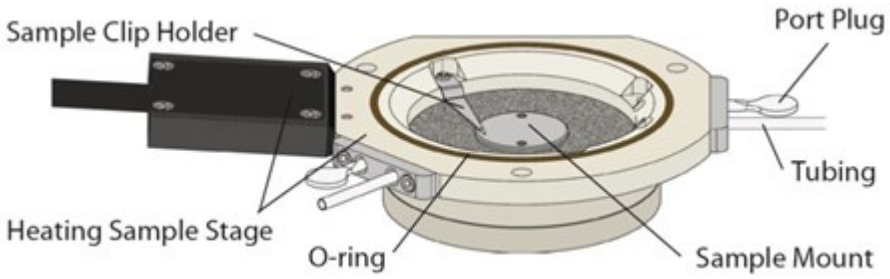

Figure 3.15: Schematic drawing of the used PolyHeaterDSHR by Asylum Research [5].

4 Preliminary tests

Preliminary charging and measurement tests were performed in order to define proper parameter settings for the rubbing and the KPFM measurements. The main questions to be answered were the accuracy of scanner repositioning after cantilever change and the robustness of the mineral particle against material loss during rubbing.

The first rubbing tests were performed by rubbing a single line with a length of 5 µm from left to right. The corresponding KPFM images before and after rubbing are presented in Figure 4.1. Apparently, a significantly larger area than just the line of contact is charged. Almost the whole 50 x 50 μm^2 area exhibits an increase in surface potential of about 1 V. However the rubbed line is clearly visible in the KPFM image (Figure 4.1b). On the left side of the line of contact is a larger spot, which is the initial contact point of the particle with the surface.

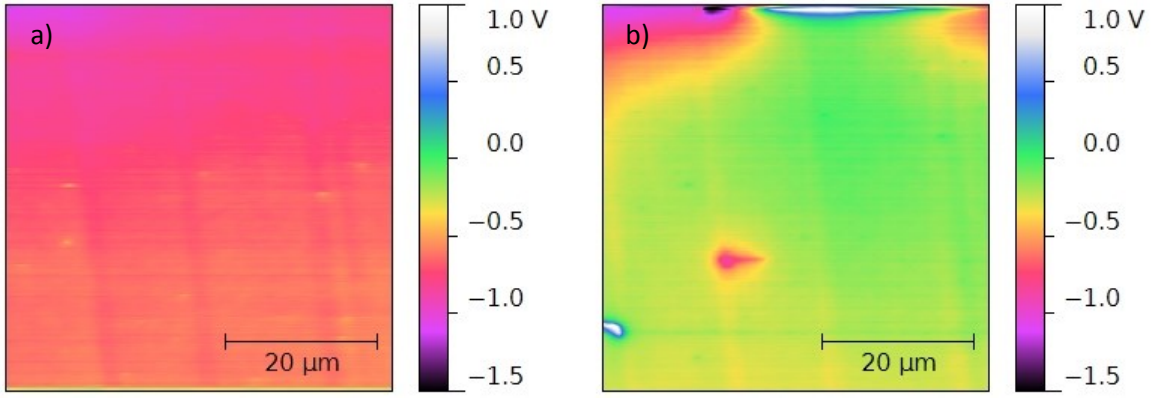

Figure 4.1: KPFM image of the $CaCO_3$(100) surface under ambient conditions: a) before rubbing; b) after rubbing a line of 5 µm.

Figure 4.2 shows the first test of rubbing a square area with a size of 5 x 5 μm^2. The KPFM image (Figure 4.2a) shows the situation before rubbing. In this case the surface exhibited a rather homogeneous potential over the whole 50 x 50 μm^2. The white line in the upper part of Figure 4.2b is most likely just an artefact originating from an unintentional contact during repositioning. On the left side of Figure 4.2b the rubbed area is well visible by a local decrease of the potential to -2 V. It is interesting that the rubbing area has indeed a defined squared shape, indicating that there is no multi point contact of the particle with the surface.

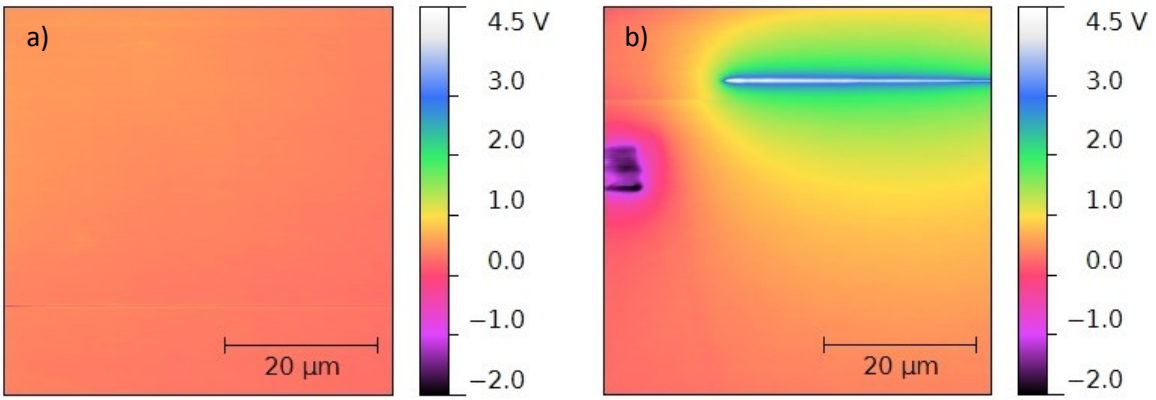

Figure 4.2: KPFM image of the $CaCO_3$(100) surface under ambient conditions: a) before rubbing;. b) after rubbing an area of 5 x 5 μm^2, a repositioning after the first scan line of the 2nd force map is the reason for the white line.

Different voltages

In order to evaluate the effect of electrostatic interaction between the AFM probe and the charged surface on FD curves were performed. For comparison, charge differences between tip and surface were “simulated” by applying a voltage to the tip [14].

The cantilever and the surface act like a capacitor. When the potential difference rises, an attractive force acts on the cantilever and it is bending towards the surface. The higher the potential difference, the stronger the cantilever is bending.

In Figure 4.3, a series of force distance curves for different tip voltages is shown. Here, a grounded metal plate was used as substrate and an NSG30/TiN conductive AFM probe was employed. In this case, the potential difference between tip and surface is well defined. The potential difference between tip and substrate was varied between 0 and 20 V. The increased bending with increasing difference is well visible in the image.

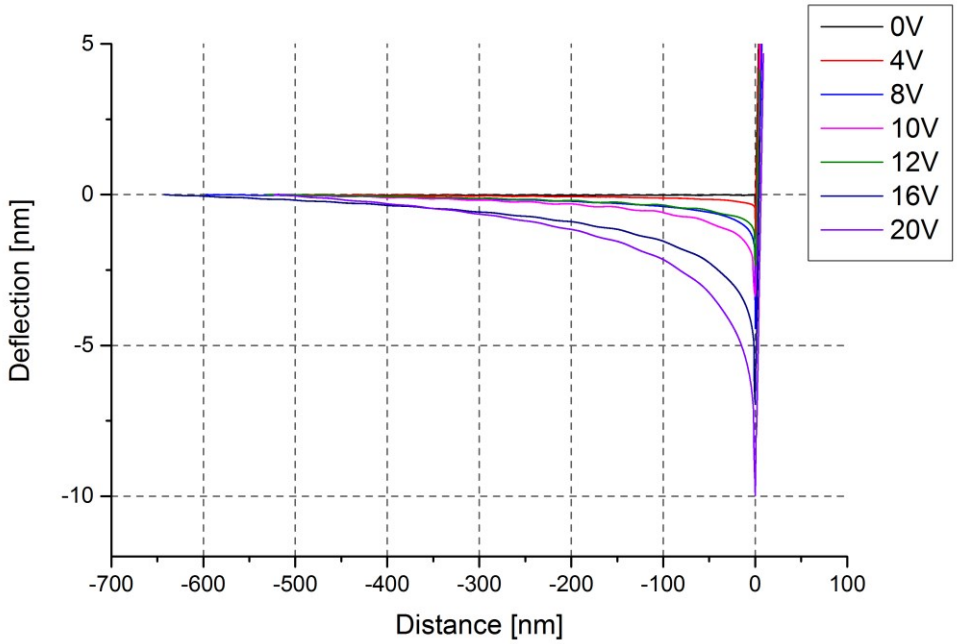

Figure 4.3: Force distance curves (approach) with a standard NSG30/TiN tip on a metal plate, with different applied tip voltages.

4.1 Measurements on calcite substrate

After the parameters for proper repositioning and rubbing were found, measurements were conducted on a $CaCO_3$(100) substrate. All measurements were performed at nearly the same conditions. The temperature was controlled with the heating stage and held at 30 °C, 40 °C, and 50 °C respectively. The relative humidity in the lab was recorded and was typically between 42 %RH and 55 %RH. Before each experiment, the samples were heated up to 130 °C for one hour, to reduce the water layer on the sample surface. This procedure is important because a water layer influences the charging effect between particle and surface. The measurements with the calcite particle were done first. Two different loading forces (0.1 µN and 0.01 µN) at all three temperatures (30 °C, 40 °C, and 50 °C) were used. The conditions for the quartz particles were the same as for calcite. However, for the quartz particles only a loading force of 0.1 µN was used rubbing with it on the $CaCO_3$(100) substrate.

4.2 Surface roughness

Knowledge about the surface roughness is important for the rubbing procedures. A smoother surface is more defined, since a rough surface might lead to an uncontrolled movement (stick-slip effect or twist) of the cantilever. Useful results can only be obtained from smooth surfaces. The surface roughness (rms-roughness for a 2-dimensional area: $R_q = \sqrt{\frac{1}{MN}\sum_{m=1}^{M}\sum_{n=1}^{N}(z_{i,j} - \langle z \rangle)^2}$ [35]) of the $CaCO_3$(100) single crystal was deducted from AFM topography images using the AFM analysis software Gwyddion [9]. The results are compiled in Table 3.

Table 4.1: Surface roughness of all samples.

Sample	RMS [nm]
30 °C; 0.01 µN – calcite	10
40 °C; 0.01 µN – calcite	4.0
50 °C; 0.01 µN – calcite	4.4
30 °C; 0.1 µN – calcite	5.9
40 °C; 0.1 µN – calcite	1.9
50 °C; 0.1 µN – calcite	6.6
30 °C; 0.1 µN – quartz	4.0
40 °C; 0.1 µN – quartz	8.2
50 °C; 0.1 µN – quartz	4.4
Mean roughness	**5.5**

Except of some occasionally present dust particles the surfaces are quite smooth. However, the dust particles are important landmarks for the repositioning after probe change.

5 Results and Discussion

5.1 Rubbing with calcite particle on $CaCO_3$(100) at 0.01 µN

The preliminary tests are not only used as feasibility study of the system. Also tests to define the parameters for the following measurements were done. This resulted in a workable analysing area of 50 x 50 µm^2 around a rubbing zone of 20 x 20 µm^2. An analysing area six times larger than the rubbing area is necessary because the rubbing with the mineral particle affects a significantly larger surface region than the rubbed area itself.

For the first rubbing experiment with a calcite particle modified AFM probe on $CaCO_3$(100) a loading force of 0.01 µN was chosen. The experiment was repeated at 30 °C, 40 °C, and finally 50 °C. Rubbing speed was about 0.1 Hz (5 µm/s) with 256 scan lines.

0.01 µN, 30 °C – calcite

In Figure 5.1, the surface morphologies before Figure 5.1a and after Figure 5.1b rubbing with a calcite particle are compared. There is no indication of surface wear. However, the rubbed area can be seen indirectly, because during the rubbing process dust particles have been pushed aside. In Figure 5.1, the dust particles used for orientation are indicated by the red ellipses. The rubbed area is indicated by the black square in Figure 5.1b.

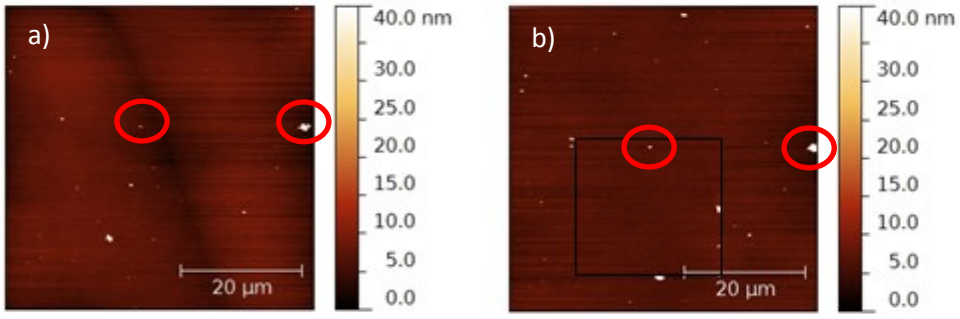

Figure 5.1: 50 x 50 µm^2 AFM height images of the surface:
a) before and b) after rubbing at 30 °C and 0.01 µN. The red circles are landmarks for the repositioning process and the black square the rubbed area.

In Figure 5.2a, the contact potential difference between AFM-tip and surface before the first contact charging experiment is shown. Interestingly, there is a large CPD difference between the top and the bottom part of the image. The sharp transition from negative to positive CPD value indicates that the measured CPD change was induced by the measurement (slow scan axis top to bottom, fast scan direction horizontal). Most likely, the tip changes due to picking up some lose material from the surface. This assumption is supported by comparison of the CPD map with the corresponding topography scan, shown in Figure 5.2. In order to investigate the electrostatic interaction between particle and substrate force maps (array of force distance curves) have been measured before and after rubbing.

In Figure 5.2b, the CPD image after the first force map before rubbing is shown. There is already a significant change in the surface potential visible. At this stage it is not clear whether this is a consequence of the time delay between the measurements or caused by the repetitive particle-substrate contact during force mapping.

Figure 5.2c shows the CPD map measured directly after rubbing a 20 x 20 μm^2 square area with the particle modified probe. The rubbing area is well visible in the bottom part of the image. Interestingly the left, the right, and the bottom rim of the rubbed area exhibit negative CPD values (0 to -0.2 V) whereas the other parts have positive CPD values up to 0.7 V The inhomogeneous CPD distribution within the rubbed area indicates an inhomogeneous charge uptake.

Apparently, also the surrounding area is influenced by the tribocharging process. Compared to the situation prior to rubbing, the CPD of the surrounding surface has dropped from 0.3 - 0.2 to 0.1 - 0.2 V. This again points towards charge redistribution over rather large distances on the surface. Again a force map has been measured on the charged surface. The corresponding CPD, recorded right after the force mapping shown in Figure 5.2d, is very similar to Figure 5.2c, indicating, that the introduced charge is rather stable in this case.

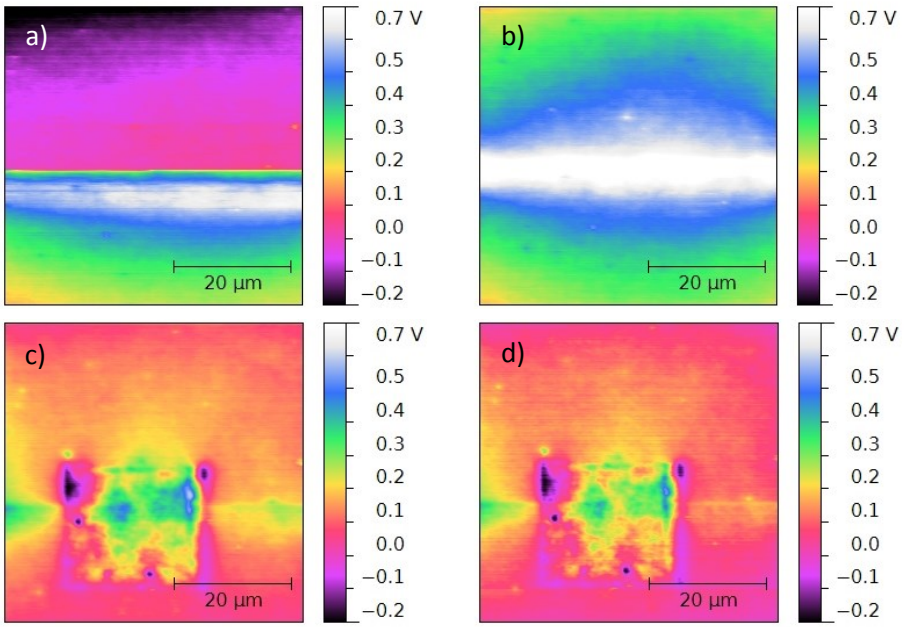

Figure 5.2: KPFM measurement rubbing with a calcite particle at 0.01 µN and 30 °C:
a) before rubbing/force mapping; b) after the 1st force map;
c) after rubbing; d) after 2nd force map.

A closer examination has to be done on the immediate change of the CPD signal (Figure 5.2a). In Figure 5.3, parts with this inhomogeneity have been enlarged in order to reveal more details. In the zoomed part of the KPFM image, a small step is visible exactly where the CPD signal changes. There, the signal jumps from 0 V to 0.7 V. In the corresponding height image a short white line (dust particle) is visible at the same position. This indicates that the tip hit and moved some material on the surface. This collision changed the tip properties which is responsible for the change in CPD signal.

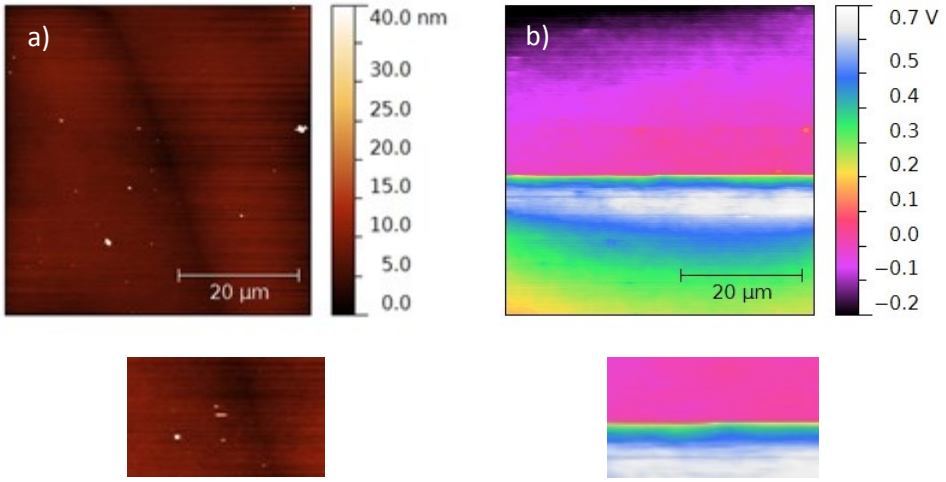

Figure 5.3: a) AFM height image and b) KPFM CPD signal of the 30 °C at 0.01 µN measurement. The masked areas have been enlarged below.

0.01 µN, 40 °C – calcite

The second measurement with 0.01 µN was performed at 40 °C. The $CaCO_3$(100) substrate was the same, but the scan position differed. The AFM height images of the sample are shown in Figure 5.4 before and after rubbing. Small indications of moved material are visible at the right rim of the rubbed area. Apart from that no sign of possible surface wear can be seen.

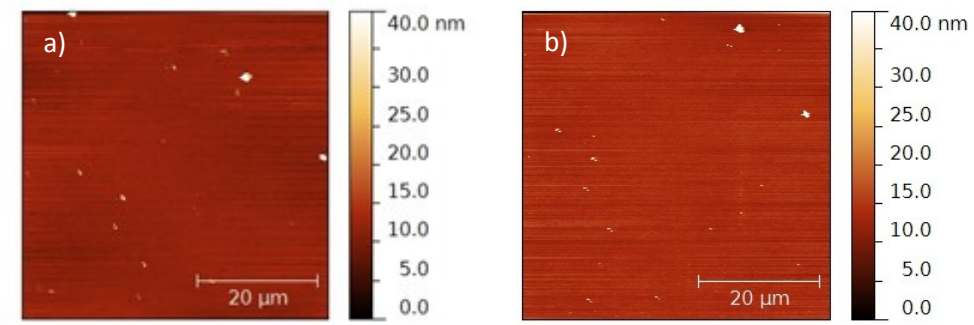

Figure 5.4: 50 x 50 µm^2 height images by rubbing with a calcite particle on $CaCO_3$(100) at 0.01 µN and 40 °C: a) flat surface with some dust particles; b) no surface wear is visible and also the dust particles are on the same place as before.

The CPD map before rubbing is presented in Figure 5.5a. The CPD is more homogeneous as compared to the 30 °C sample with 0.01 µN. There is no abrupt change of surface potential. Only a small gradient from top to bottom in the slow scan direction from +0.2 V to -0.3 V is visible.

After the first force map measurement only small changes in CPD are observed in Figure 5.5b. However, the potential gradient has vanished, the CPD has an almost constant value of about -0.4 V. Only in the bottom right corner the potential drops a little bit to -0.5 V.

The situation after surface charging is shown in Figure 5.5c. The rubbed area is well visible in the center of the investigated area. The shape is as expected a square, but the potential is not constant. While the top center part has a CPD of -1.4 V, there is a potential variation towards the rims. The left, the bottom, and the right rim are less charged. The left rim shows no change in CPD compared to Figure 5.5b (-0.4 V), whereas the other two change to -1.0 V.

Again, the surrounding area is also affected by the charging. The influence of the rubbing with the modified tip reaches out much further than the 20 x 20 µm^2 rubbed area. The surface potential of the surrounding area drops to -0.7 V and indicates a charge spread.

The last image of the measurement sequence (Figure 5.5d) shows the surface after the second force map. The CPD value increases, not only for the rubbed area, but also for the

rest of the investigated area. The CPD value of the rubbed area in Figure 5.5d increases to -0.9 V, the surrounding to -0.3 V. Similar charge decay is also observed of the previous measurement with 30 °C.

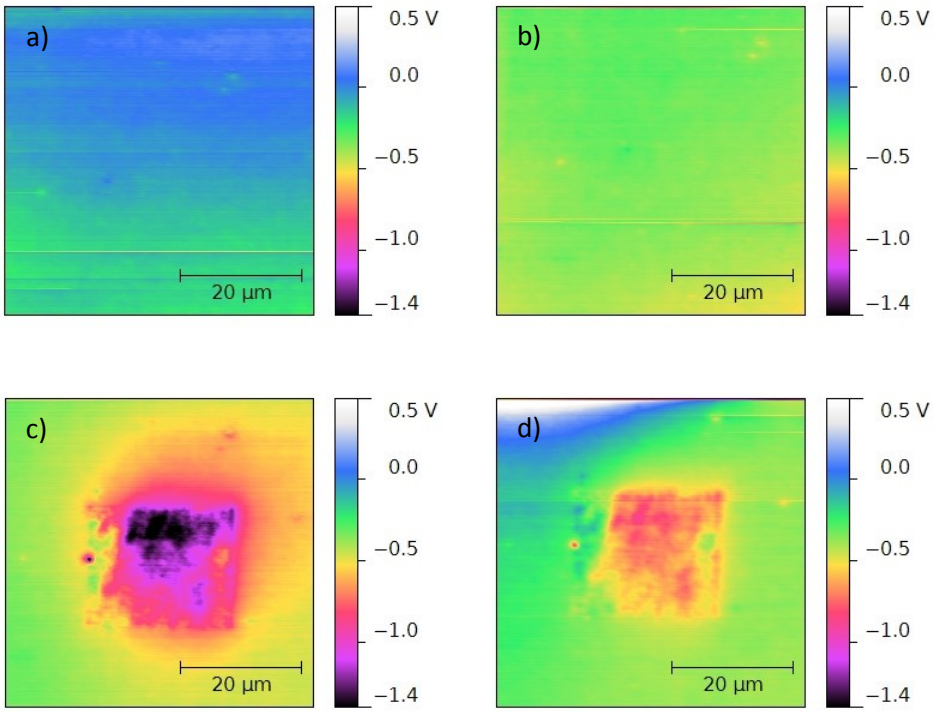

Figure 5.5: 50 x 50 µm^2 KPFM measurement rubbing with a calcite particle at 0.01 µN and 40 °C: a) small gradient in surface potential in both scan directions (fast and slow scan); b) homogeneous CPD of -0.4 V after the 1st force map; c) the rubbed area presents a negative charged center and low charged rims; d) after 2nd force map the CPD of the surround changed back to the pristine value and the charged 20 x 20 µm^2 present a strong increase.

0.01 µN, 50 °C – calcite

The behaviour of the rubbed surface at 50 °C is similar to the other 0.01 µN measurements at lower temperatures. The height images in Figure 5.6 show again moved dust particles but no surface wear. However, quite all particles get moved on this sample. Only one triangular shaped particle is visible on both images, making recognition of the area possible.

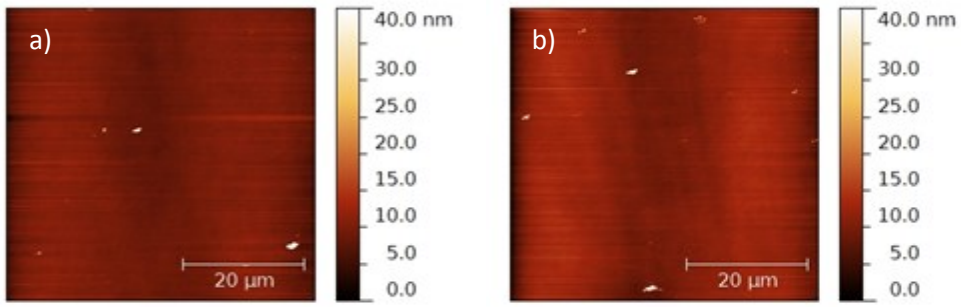

Figure 5.6: 50 x 50 µm^2 AFM height images of the surface rubbed with 0.01 µN at 50 °C: a) initial surface; b) only one triangular shaped particle confirms the scan position after rubbing.

The situation of the surface potential before the charging process is shown in Figure 5.7a. There is a small gradient from the top right to the bottom left corner, the CPD varies from -1 V to 0 V. The exception is a single point with 0 V at the top.

After the 1st force map, the signal raises by about 0.5 V. Interestingly the overall potential goes not higher than 0.2 V. A gradient from the top right to the lower left is still present.

Figure 5.7c shows the CPD map measured directly after the rubbing. The rubbed area is well visible in the lower left corner of the image. It has a bipolar square shape and exhibits a CPD in scan direction from left (1.2 V) to right (-1.2 V).

After a second force map sequence, the CPD is measured a fourth time. The charge is not stable, strong changes were visible between Figure 5.7c and Figure 5.7d. The whole area, the rubbed and the surface potential itself show an increased value between 0.5 V and 1 V.

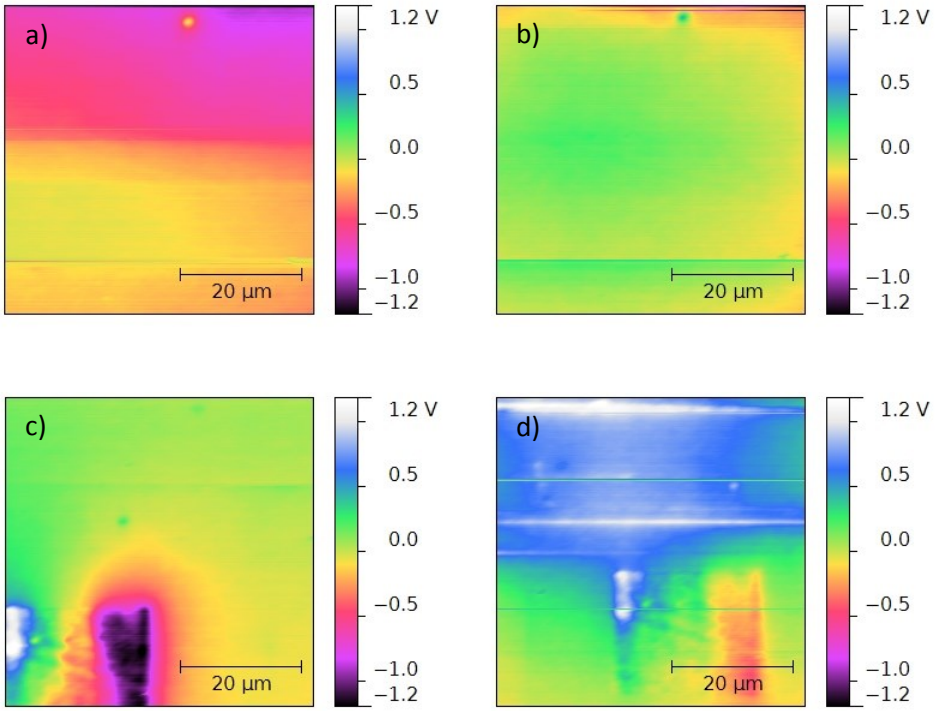

Figure 5.7: KPFM measurement rubbing with a calcite particle at 0.01 µN and 50 °C: a) the working face has a slight negative potential; b) after the 1st force map the CPD raises about 0.25 V; c) the rubbed area is on the lower left part of the image and has a bipolar shape in fast scan axis; d) the 2nd force leads to a CPD increase of 1 V of the upper part, the lower presents only the CPD change over time effect of the rubbed area.

Summarized results of rubbing with calcite at 0.01 µN on $CaCO_3$(100)

The effects of the mechanical rubbing on the $CaCO_3$(100) surfaces are similar for all temperatures applied (30 °C, 40 °C, and 50 °C). Rubbing with a calcite particle at 0.01 µN on a $CaCO_3$(100) surface leads to no visible surface wear. Also the force maps have no detectable influence on the surface morphology. However, the original surface potential (before rubbing) varied for the different measurements (between+0.3 V and -0.4 V). Nevertheless, the rubbing resulted in significant change of the local surface potential for all measurements indicating the build-up of surface change. In Figure 5.8, three diagrams show the trends for the CPD value in the different states of the measurement sequence.

The black line is the averaged potential of the whole measures 50 x 50 μm^2 area, which includes the rubbed area. The red line is the average value of the rubbed area alone and the blue one is the value for the whole scanned region without the rubbed area. The extraction of the surface potential for the rubbed area and for the scanned area without the rubbed one allows a better understanding of the influence of the rubbing process.

In all KPFM images of the different measurements, a charging of the near surrounding of the rubbed area is visible. This effect is presented in the difference of the blue and the black line. On the measurement with 0.01 µN at 40 °C the charging effect of the surrounding is stronger than on the measurements at 30 °C and 50 °C. In comparison to the KPFM images of the different measurements, this observation is convenient. Another effect, which is well visible on these diagrams, is the influence of the rubbing with a mineral particle on a $CaCO_3$(100) surface. On all three diagrams, the rubbing with a calcite particle leads to a decreasing of the CPD signal of the surface. Force mapping has also a strong influence to the surface potential.

A closer look to these results is given in chapter 6.3 (charging with the particle) and chapter 6.4 (influence of the force map).

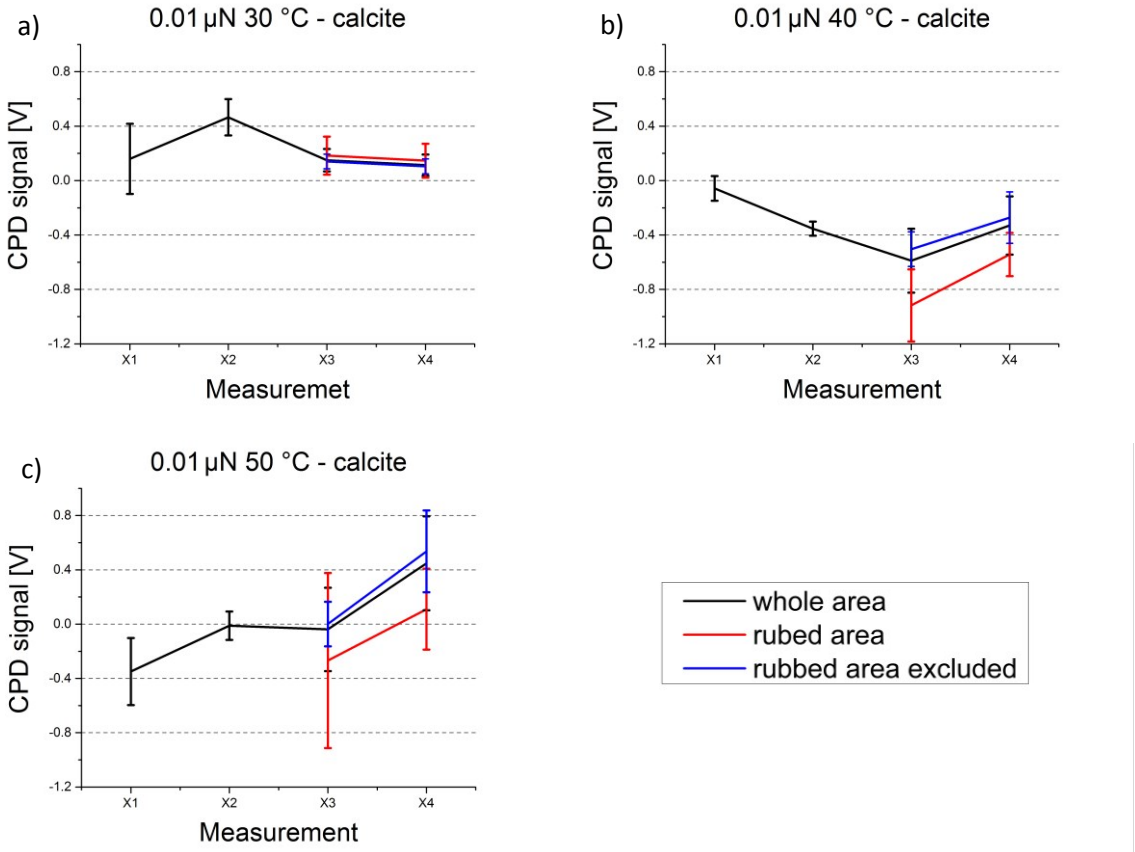

Figure 5.8: Average CPD by rubbing with calcite on $CaCO_3$(100) at 0.01 µN and a) 30 °C, b) 40 °C, and c) 50 °C. These are the situations at the beginning of the measurement (X1), after the first force mapping (X2), after rubbing with the modified tip (X3) and the situation at the end of the measurement sequence (X4).

5.2 Rubbing with calcite particle on $CaCO_3$(100) with 0.1 µN

The first series of rubbing experiments with a calcite particle on a $CaCO_3$(100) surface were done with three different temperatures (30 °C, 40 °C, and 50 °C) and with one defined force (0.01 µN). This small force is enough to see a changing in CPD of the surface in the investigated area. To see the influence of the force to the measurements, the second series was done with the same three temperatures but with different force. For this second measurement the force was changed to a ten times higher value, 0.1 µN.

0.1 µN, 30 °C – calcite

The second series starts again with the 30 °C measurement, the second will be at 40 °C and the third with 50 °C. Two AFM height images Figure 5.9a before and Figure 5.9b after rubbing with 0.1 µN are presented. The surface shows no indications of surface wear even for the high force. Just a small scratch on the lower right corner appeared after rubbing. A small shift in y-direction is visible, but the scan position is nearly the same after rubbing.

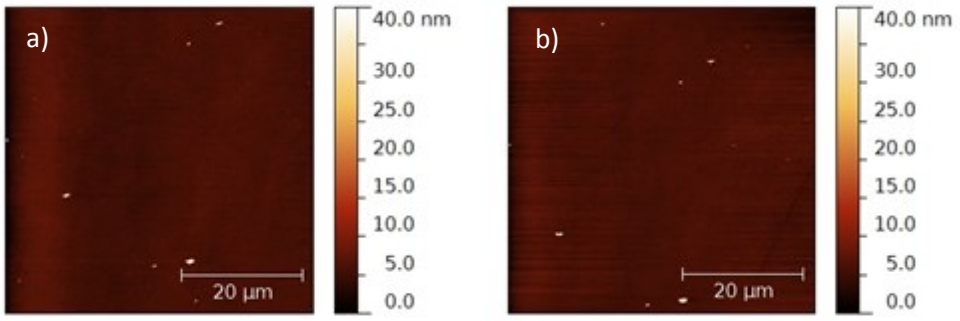

Figure 5.9: 50 x 50 µm^2 AFM height images of the surface 0.1 µN and 30 °C:
a) working face before the 1st force map; b) after rubbing is a scratch on the lower left visible, which is not present on the pristine surface.

The first KPFM image in Figure 5.10a shows the surface potential prior to the first charging experiment. Normally, the pristine surface has a CPD signal near 0 V. Here, it shows a negative charge of about -6 V. A small change of 0.5 V is visible near the middle of the image. Such a change in CPD signal can happen when the tip is picking up in some loose material from the surface. Here, this effect is small in comparison to strong CPD change of the previous measurement with 0.01 µN and 30 °C.

In Figure 5.10b, two blue lines are visible at the top of the image. It was necessary to restart the force mapping sequence after two scan lines, because of a sudden shift of the

scan area. Therefore, these two blue lines are the result of an aborted force mapping sequence and a repositioning in x-direction. This statement can be confirmed by measuring the distance between these two lines and the fact, that the force map was restarted again. The surface potential rises by about 2 V after the restarted force map was completed. A larger change is visible around the two aborted scan lines. The explanation for this effect is that the CPD of these lines were changed twice.

Figure 5.10c shows a light position difference in x- and y-direction compared to the first KPFM measurements. The rubbing area is on the left side of the scanned region. Again there is a strong gradient in scan direction from left to right. A similar observation was made on the sample 0.01 µN and 50 °C. Here, the left side is also positive and the right side has a negative charge (bipolar shape). The charge difference is in total 11 V (between left and right side of the rubbed area). 2.5 V positive on the left and -8.5 V on the right. The surrounding area of the negatively charged side is also affected.

On Figure 5.10d the x- and y-position were changed again after the 2nd force map step to enable a better a whole view of the rubbed area. Here, the decrease of the CPD is larger than in the former experiments. This might be the case because the initial surface potential was also significantly higher in this case.

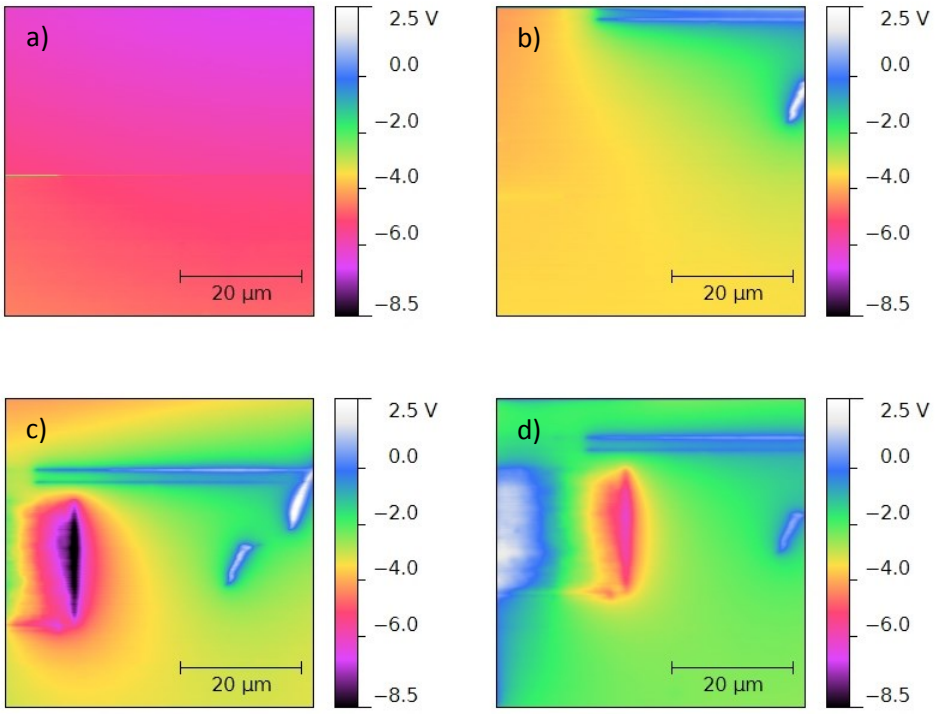

Figure 5.10: 50 x 50 µm^2 CPD map rubbing with a calcite particle at 0.1 µN and 30 °C: a) before rubbing/force mapping; b) the two blue lines in the top present a reposition of the force map after the first two scan lines; c) the rubbed area has a bipolar shape; d) a reposition of the scan area has to be done to get a whole view onto the rubbed area.

0.1 µN, 40 °C – calcite

The AFM height images in Figure 5.11 show the morphology situation before Figure 5.11a and after Figure 5.11b rubbing a 20 x 20 µm^2 square area. During the measurement sequence, dust particles were pushed aside. Often dust particles vanish in the course of the measurement, because they are pushed out of the scanned area or just picked up by the tip. Interestingly, in Figure 5.11b after rubbing are more particles visible than in image Figure 5.11a.

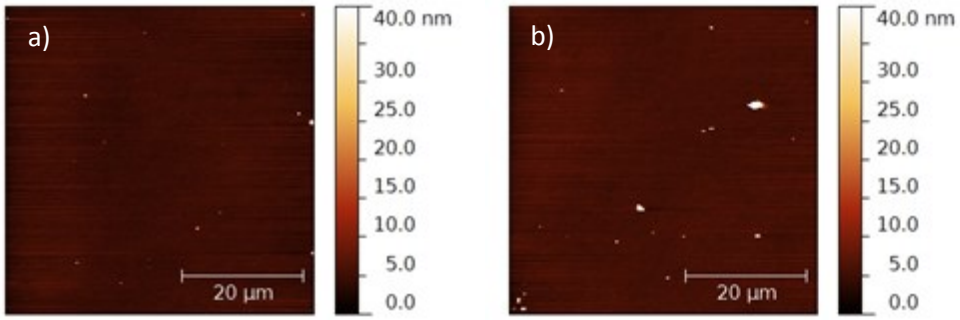

Figure 5.11: AFM height images of the surface rubbing with calcite at 0.1 µN and 40 °C: a) clean flat surface at the start of the measurement; b) more dust particles are visible after the rubbing process.

Figure 5.12a shows a very homogeneous KPFM signal before the first contact charging experiment is done. The surface itself is inconspicuous, a very small gradient between the top and bottom in the slow scan direction is visible. The highest value is 1.5 V of the bottom left and the lowest 1 V at the top right corner.

The only change from Figure 5.12a to Figure 5.12b is a slight increase of the surface potential by 0.2 V over the whole area. In this image it is again not clear if this change is a consequence of the force map or if it is a time effect.

Figure 5.12c, the KPFM measurement directly after the rubbing shows the expected square shaped rubbed area. The central part has the lowest CPD of -2.5 V. To the rims the CPD raises up to -1.5 V. The area with changed CPD (charged region) is larger than the area of mechanical contact (rubbed area) indicating a spread of the charge on the insulating surface. As well visible in Figure 5.12b, the CPD signal gradually goes back to its initial value. The influenced area is extending by about 20 µm around the rubbed area.

The fourth KPFM measurement (Figure 5.12d) shows the situation after the second force map. The earlier experiments show a change of the potential of the rubbed and the surrounding area after the second force map. The same can be observed on this sample. Here, this effect is still visible after the 2nd force map. While the CPD within the rubbed area

increases by +1 V between Figure 5.12c and Figure 5.12d, the potential of the initial surface stays constant at +1.5 V.

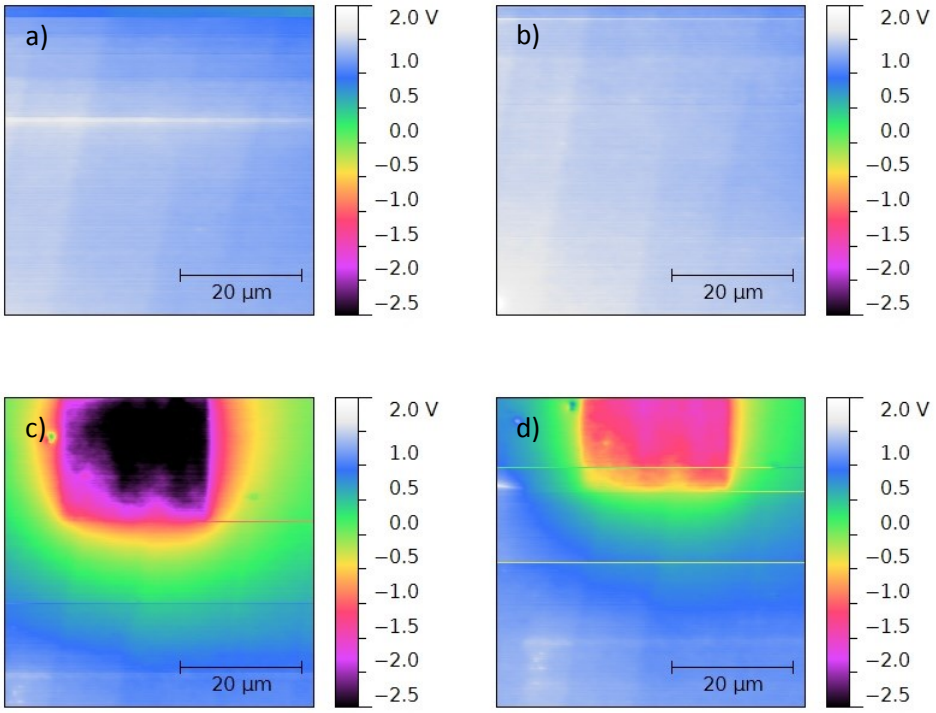

Figure 5.12: 50 x 50 µm^2 KPFM measurement rubbing with a calcite particle at 0.1 µN and 40 °C: a) small gradient in surface potential from top to bottom is visible; b) the 1st force map leads to no change in surface potential; c) a rubbed area with a nearly perfect homogeneous negative charge is presented in the top half; d) the charge of the surrounding is not totally gone after 2nd force map.

0.1 µN, 50 °C – calcite

In Figure 5.13, a comparison of the surface morphology before and after rubbing is presented. The AFM height image before rubbing reveals the presence of quite a lot of dust particles. In comparison to the situation before (0.1 µN and 40 °C), the surface after rubbing is much cleaner. This cleaning effect is the result from particle removed by the AFM probe. During the subsequent modification and measured steps, the AFM tip can pick up a particle or push it to the rims of the scanned area. This leads to a locally cleaner surface after the measurements.

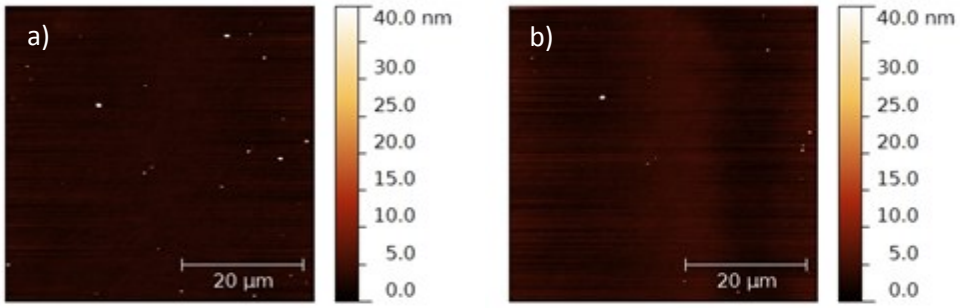

Figure 5.13: 50 x 50 µm^2 height images rubbing with calcite on $CaCO_3$(100) at 0.1 µN and 50 °C: a) initially some small dust particles are on the surface; b) cleaned surface after force map and rubbing than before.

Figure 5.14a represents the surface potential before the first force map. Here, a rather homogeneous surface with a potential between 0 V and 0.5 V over the whole area is visible. There are also three scan artefacts in form of single horizontal lines, one on the top and two in the middle. There the tip interacted with some lose material on the surface.

Figure 5.14b is unique, it is the only image where the single interaction points between the tip and the surface are directly visible in KPFM. Force map represents 32 x 32 FD curves performed on a quadratic raster. In every single FD measurement the tip and the surface come into contact. These contacts cause a positive CPD change on every single of the 1024 touching points which are observed. Also apparent is the combined potential of the single charged points. The CPD in the center is higher than on the rims. Therefore the electric potential gradually drops from 2 V in the center to 0.7 V at the corners.

Figure 5.14c presents the situation directly after the rubbing sequence with the modified tip. The rubbing area is well visible on the bottom right part of the image. Exceptional is the shape of the rubbed area. It looks like three single columns with a common base. The CPD of the rubbed base dropped to 0 V whereas the three columns exhibit a CPD of 0.5 V. In this case no influence on the potential of the surrounding surface is visible, the remaining surface has the same value of 1 V to 2 V like before.

Again, a force map has been measured on the charged surface. The corresponding CPD recorded right after the force mapping shown in Figure 5.14d is very similar to Figure 5.14c indicating that the charge introduced by rubbing is rather stable in this case. Only the potential of the surface with the charged point raster decrease slightly by ~0.2 V.

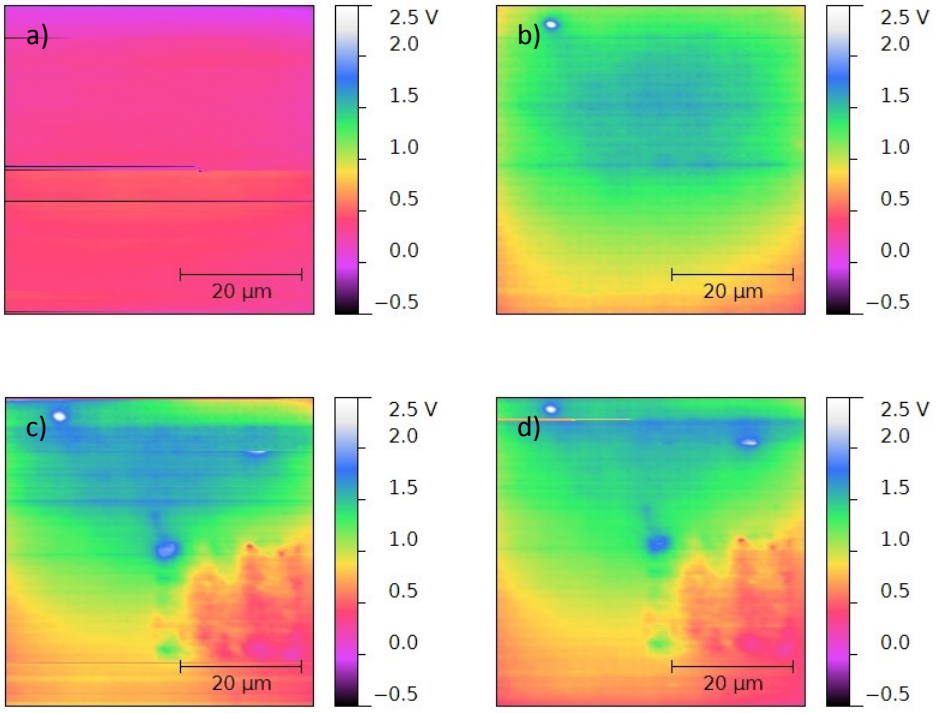

Figure 5.14: KPFM measurement rubbing with a calcite particle at 50 °C and 0.1 µN: a) before rubbing/force mapping; b) FD touching points are visible after the 1st force map; c) rubbed area in the lower right; d) a small change of CPD of the touching points, but none of the rubbed area.

Results of rubbing with constant force of 0.1 µN calcite on $CaCO_3$(100)

The different developments of the averaged CPD signal when rubbing a calcite particle on a $CaCO_3$(100) with 0.1 µN are presented in Figure 5.15.

These measurements with the calcite particle exhibit also a decreasing of the CPD signal (black line from X2 to X3) like the measurements with a force of 0.01 µN did. It is not necessary if the surface has a positive or negative potential before the rubbing process, the rubbing with calcite leads to a more negative CPD. Here, the force mapping has a stronger influence on the surface than the measurements with calcite at 0.01 µN.

A closer look to these results is given in chapter 6.3 (charging with the particle) and chapter 6.4 (influence of the force map).

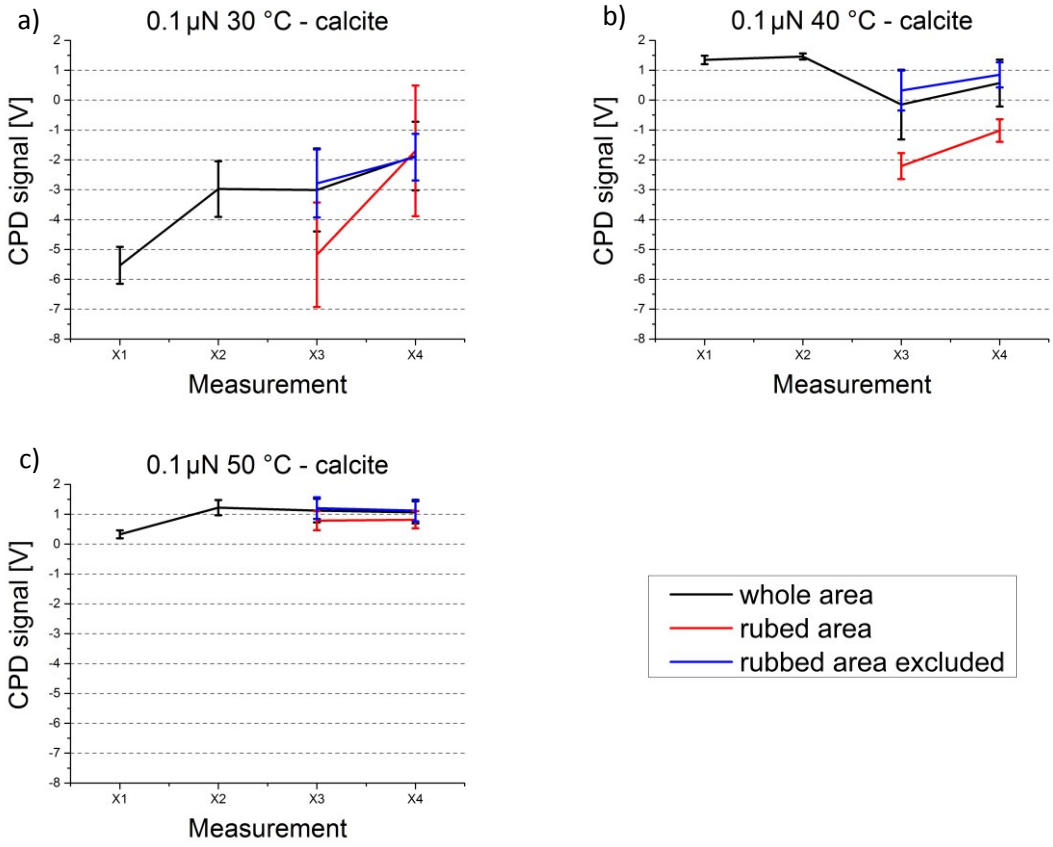

Figure 5.15: Contact potential difference for calcite rubbed on $CaCO_3$ at 0.01 µN contact force and a) 30 °C, b) 40 °C, and c) 50 °C. X1, X2, X3 and X4 are the situations before the 1st FM, after the 1st FM, after the rubbing with the particle and at the end of the measurement sequence.

5.3 Rubbing with quartz particle on $CaCO_3$ surface with 0.1 µN

The first two sets of investigations were made with a calcite particle modified NSG30/TiN probe at two different forces (0.01 µN and 0.1 µN). A change of the rubbing particle material on the same $CaCO_3$(100) surface is another parameter to influencing the surface charging. Quartz and calcite are both minerals. They have different mechanical and electrical properties. The interesting fact about these two minerals is that the separation process to get powders with high purity is the same for both materials. Therefore, quartz is an interesting material for comparison with calcite. Thus, cantilevers with attached quartz particles have been prepared as described in chapter 3.3. Rubbing experiments on $CaCO_3$(100) have been performed at a force of 0.1 µN at 30 °C, 40 °C, and 50 °C.

0.1 µN, 30 °C – quartz

The AFM height images in Figure 5.16 reveal differences in morphology of this scan position compared to the measurements performed with a calcite particle before. There are two big scratches in the surface, one from top to bottom, and the other from left to right, which could be used for orientation (Figure 5.16a). After the 3rd KPFM measurement it was necessary to shift the scan position to obtain a whole view on the rubbed area.

The rubbed area can be recognized indirectly in Figure 5.16c, because during the rubbing process material is pushed aside. This effect is more pronounced for quartz rubbing on $CaCO_3$(100), compared to calcite on calcite. A possible explanation is the difference in hardness of the minerals (Quartz: Mohs hardness 7; Calcite Mohs hardness 3 [11]) which causes surface wear on the softer calcite substrate.

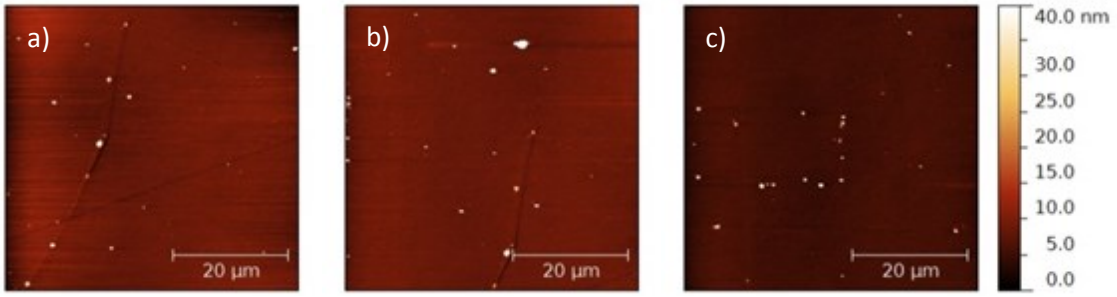

Figure 5.16: AFM height images of the surface rubbing with quartz at 0.1 µN and 30 °C: a) start of the measurement with two visible scratches; b) after the rubbing process; c) reposition, because of a shift of the rubbed area with much surface wear around the rubbed area.

Figure 5.17, represents the CPD map of the pristine surface before the first contact charging experiment. The surface exhibits a smooth and homogeneous potential near 0 V. In the topography image of Figure 5.16a, there are two large scratches visible, one from top to bottom and a second from left to right. Interestingly, the scratches are not visible in the KPFM images. Normally, a simple touch with a dust particle is sufficient to change the local potential of the surface a little bit, but in this measurement, surface irregularities seem to have no influence on the surface potential.

The KPFM image in Figure 5.17b shows the surface potential after the first force map step. The CPD value stayed unchanged in this case, thus the surface remains uncharged indicating that force mapping and KPFM measurements have no influence on the surface potential.

Figure 5.17c represents the CPD map measured directly after the rubbing sequence. The overall surface shows CPD values ranging from 2 V (top) to -0.3 V (bottom). Interestingly,

directly outside of the left and the right rim of the rubbed area are pronounced negative CPD values (up to -1.5 V) whereas the central rubbed part has positive CPD values up to +1 V. The charging process with quartz also seems to influence the surrounding area.

The change of CPD between Figure 5.17c and Figure 5.17d is remarkable. All areas show a CPD drop of about -0.7 V, except the two negative elongated areas near the left and right rim of the rubbed area presents a stable surface potential.

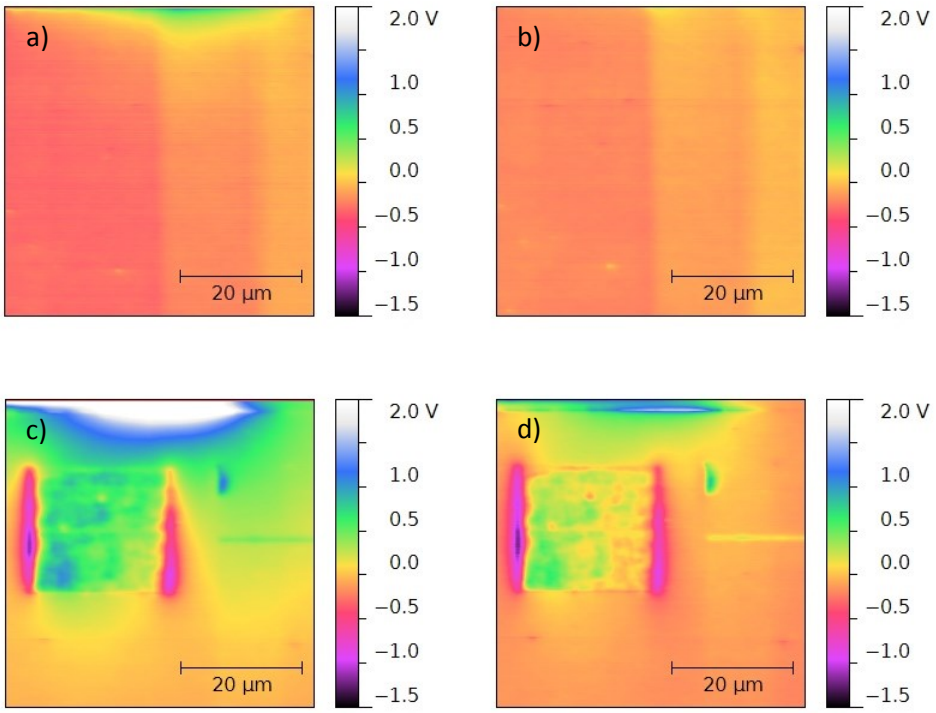

Figure 5.17: 50 x 50 µm^2 KPFM measurement rubbing with a quartz particle at 0.1 µN and 30 °C: a) initial surface (in comparison to the topography image is no scratch visible); b) no changes in CPD after the 1st force map; c) the rubbed area exhibits two strong negative areas on the left and right rim; d) after the 2nd force map with a strong CPD change over time.

0.1 µN, 40 °C – quartz

Figure 5.18 shows the AFM height images before and after the rubbing process. In Figure 5.18b, surface wear is clearly visible. There are many particles pushed aside to the right rim of the rubbed area. The three dust particles near the bottom rim of the rubbed area are no surface wear or pushed dust particles because they do not change their position between Figure 5.18a and Figure 5.18b. A large scratch in the surface from the lower left to the upper right side is visible, it runs below the rubbed area and does not cross it.

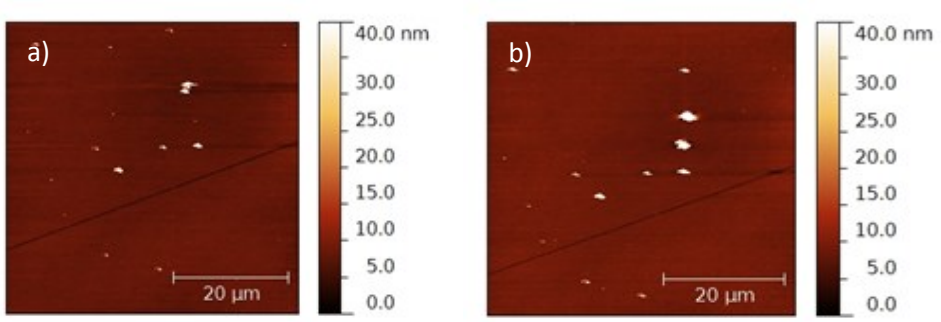

Figure 5.18: 50 x 50 µm^2 AFM height images rubbing with a quartz particle at 0.1 µN and 40 °C. a) surface with some dust particles before rubbing; b) after rubbing is surface wear visible on the right and the bottom rim of the rubbed area.

The KPFM image in Figure 5.19a present the situation before the first force map and rubbing a 20 x 20 µm^2 square have been done. A constant potential around -0.2 V is visible all over the area. This situation is comparable to the measurement with a quartz particle at 30 °C, where initially also a rather constant surface potential was observed. Figure 5.19b reveals no influences of the force map on the surface potential.

In Figure 5.19c, the results of the charging process done by rubbing with the modified tip, are shown. The rubbed area is at the top of the examined region. Here, the rubbed area has again a bipolar shape with a positive left and a negative right part. The difference of the CPD value between left and right edge is in total 10 V, up to 5 V in the positive and down to -5 V in negative direction. Again, the potential of surrounding area has also changed. The differences of the positive and negative charges are well visible. At the lower parts, several 10 µm away from the rubbed area, the potential remained unchanged at ~0.2 V.

The KPFM image of Figure 5.19d shows a large change of the CPD. In comparison to the situation prior to the second force map (Figure 5.19c) the area with positive potential exhibits a significantly larger change than the parts having negative potential. The highest positive potential is now around 2 V and the lowest negative around -4.5 V. The same trend is visible in the surrounding region. The potential values around the positive parts have returned to their initial values, whereas on the negative side the areas adjacent to the negative part are still at lower potential.

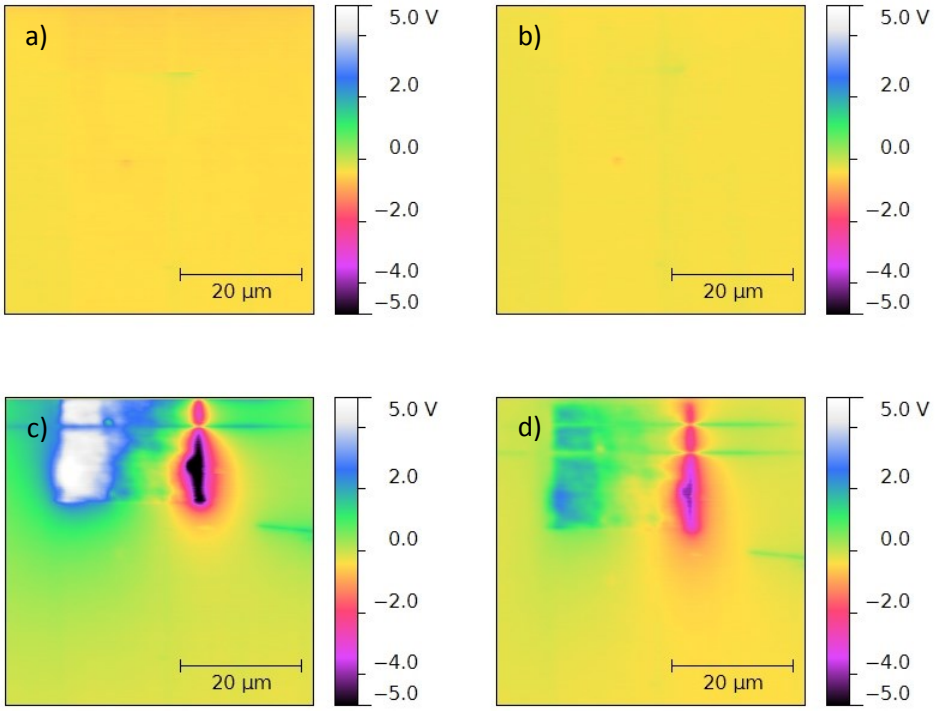

Figure 5.19: 50 x 50 µm^2 CPD map rubbing with a quartz particle at 0.1 µN and 40 °C: a) before rubbing/force mapping; b) no change in CPD after the 1st force map; c) rubbed bipolar area in the upper part of the KPFM image; d) strong CPD change of both parts (the positive as well as the negative) after 2nd force map.

0.1 µN, 50 °C – quartz

Figure 5.20 present the surface morphology of the rubbing experiment with a quartz particle at 50 °C. A small scratch and a couple of particles are visible. In Figure 5.20b, like in all other rubbing experiments with quartz (at 30 °C and 40 °C), the rubbed area is indirectly visible, because of an accumulation of particles at the edges of the rubbed area. In contrast to the previous experiments the particle concentration is highest at the top and the right rim of the rubbed area. Usually they accumulate preferentially at the bottom and the right rim, since the slow scan direction is always top to bottom. Here, the scan direction was also top to bottom, this can be confirmed with the original data's from the rubbing experiments, but interestingly the accumulation process is different.

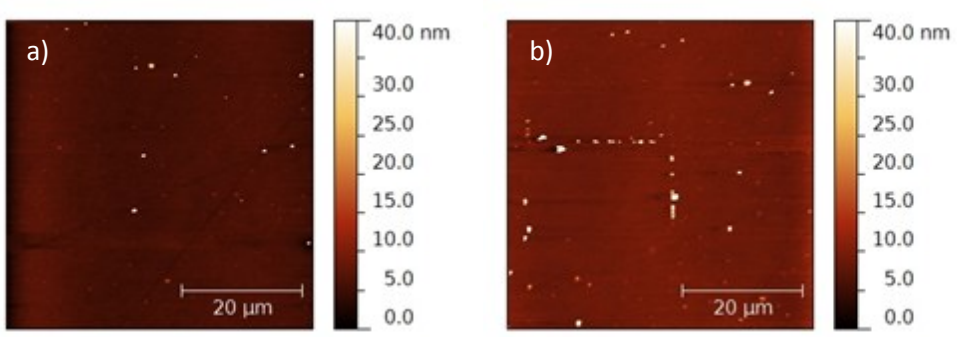

Figure 5.20: AFM height images of the measurement rubbing with a quartz particle at 0.1 µN and 50 °C: a) surface at the start of the measurement; b) surface with accumulated particles on the top and the right rim after the rubbing process.

In Figure 5.21a, the CPD distribution before the first charging experiment is shown. The surface potential of this scan position has a small gradient from the top right (-0.5 V) to the lower left (-0.3 V) corner. Here, also no influence of the surface irregularities on the CPD has been noticed.

The CPD map at the surface after the first force map is shown in Figure 5.21b. The map looks similar to that presented in Figure 5.21a, but the potential raised about 0.2 V everywhere. In general, the surface exhibits a homogeneous, featureless CPD.

The rubbed area is presented in Figure 5.21c on the lower left of the reviewed area. There are only 5 µm of the right part of the rubbed area visible, but the shape is recognizable, a negatively charged right rim and a more positive central part.

For the last KPFM image, presented in Figure 5.21d the scan position was corrected by around 20 µm in negative x-direction (to the left). Now the shape is completely visible, it reveals a positively charged left rim and the known negative right rim. It is different to the other observed bipolar shapes because the gradient between the right and the left rim distribute not even. It is more similar to the shape which was measured in the experiment rubbing with calcite at 0.01 µN and 40 °C. Furthermore, Figure 5.21d exhibits like many other measurements, a potential change over time dependence.

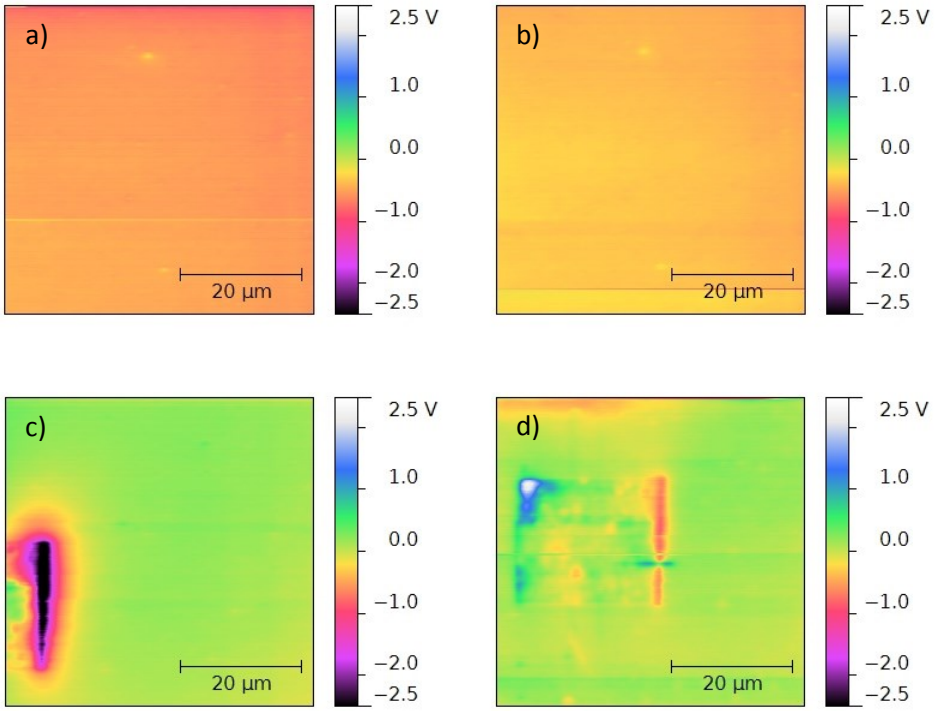

Figure 5.21: KPFM measurement rubbing with a calcite particle at 50 °C and 0.1 µN: a) working face before rubbing/force mapping; b) a small increase of CPD in comparison the working face; c) a small offset between the rubbed and the investigated area; d) a shift in x-direction to analyse the whole rubbed area.

Summary of the results of rubbing with quartz at 0.1 µN on $CaCO_3$(100)

Figure 5.22 compares the average CPD values. The big difference compared to the measurements with the calcite particle is the sign of the potential change because of the rubbing. The rubbing with a quartz particle leads to an increase of the CPD, whereas, the calcite particle decreases the surface potential. The influence of the force mapping on the CPD is quite interesting. All of them show a tendency towards a CPD of 0 V. At this point this behaviour cannot be explained. Maybe, the repetitive tip-sample contact during force mapping causes a partial discharging of the surface.

A closer look to these results is given in chapter 6.3 (charging with the particle) and chapter 6.4 (influence of the force map).

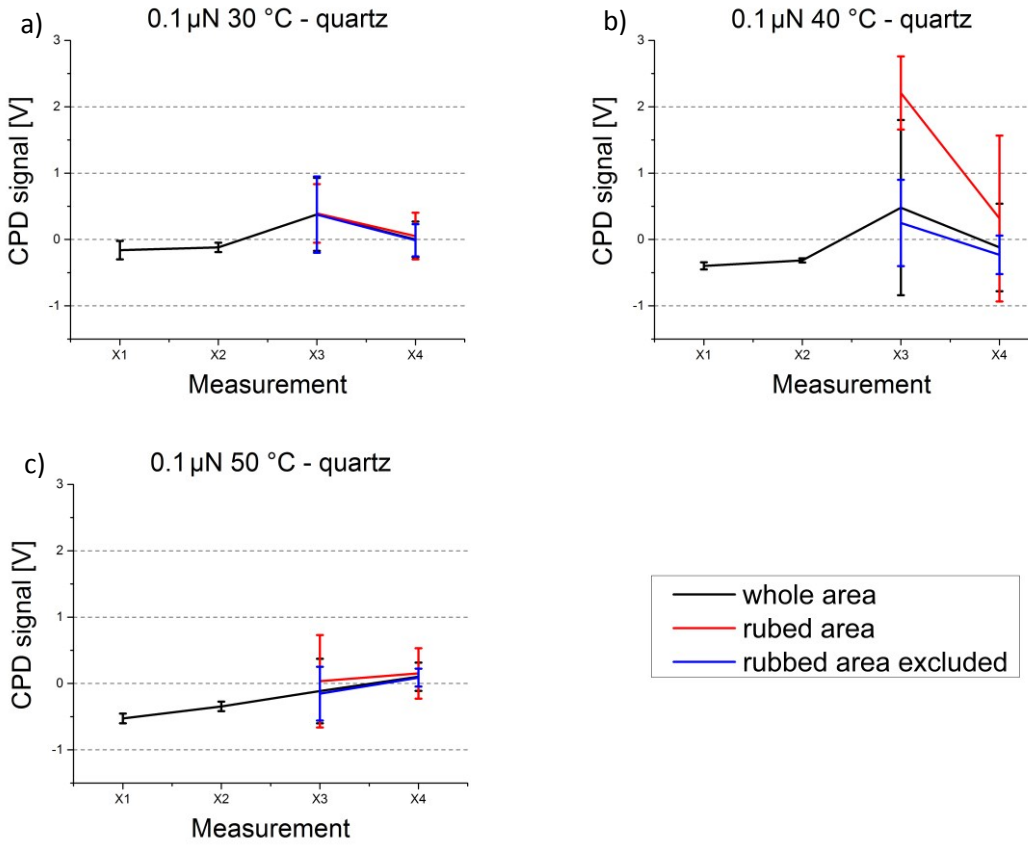

Figure 5.22: Average contact potential difference for $CaCO_3$(100) rubbed with quartz a contact force of 0.1 µN and a) 30 °C, b) 40 °C, and c) 50 °C. X1 stands for the situation at the beginning of the measurement, X2 for the situation after the first force mapping, X3 is after the rubbing with the modified tip and X4 at the end after the second force mapping.

5.4 Evolution of CPD signal with time

Most of the measurements reveal change in CPD value over time. This is not necessarily connected to rubbing but it is a consequence of charge decay. The loss of charge can be due to surface conductivity but also due to the influence of the measurements.

The effect of three different measurements, are presented in Figure 5.23. The left column is the situation directly after rubbing a 20 x 20 μm^2 square area with the particle modified tip, the right column is the surface potential after the second force mapping step. The shape of the rubbed area is slightly different, but nevertheless the CPD change is visible in all of them.

Besides the KPFM measurement itself, there are two additional effects acting on the surface between the left and the right KPFM images in Figure 5.23. The first effect is the influence of the force map sequence. 32 x 32 force distance curves were executed and this

results in 1024 individual contact points between the tip and the surface. The second effect is the natural time dependent loss of charge between these two measurements (1.25 h measurement time + 15 min. force map).

This is not necessarily connected to rubbing but is a consequence of charge decay. The loss of charge can be due to surface conductivity but also due to the influence of the measurement.

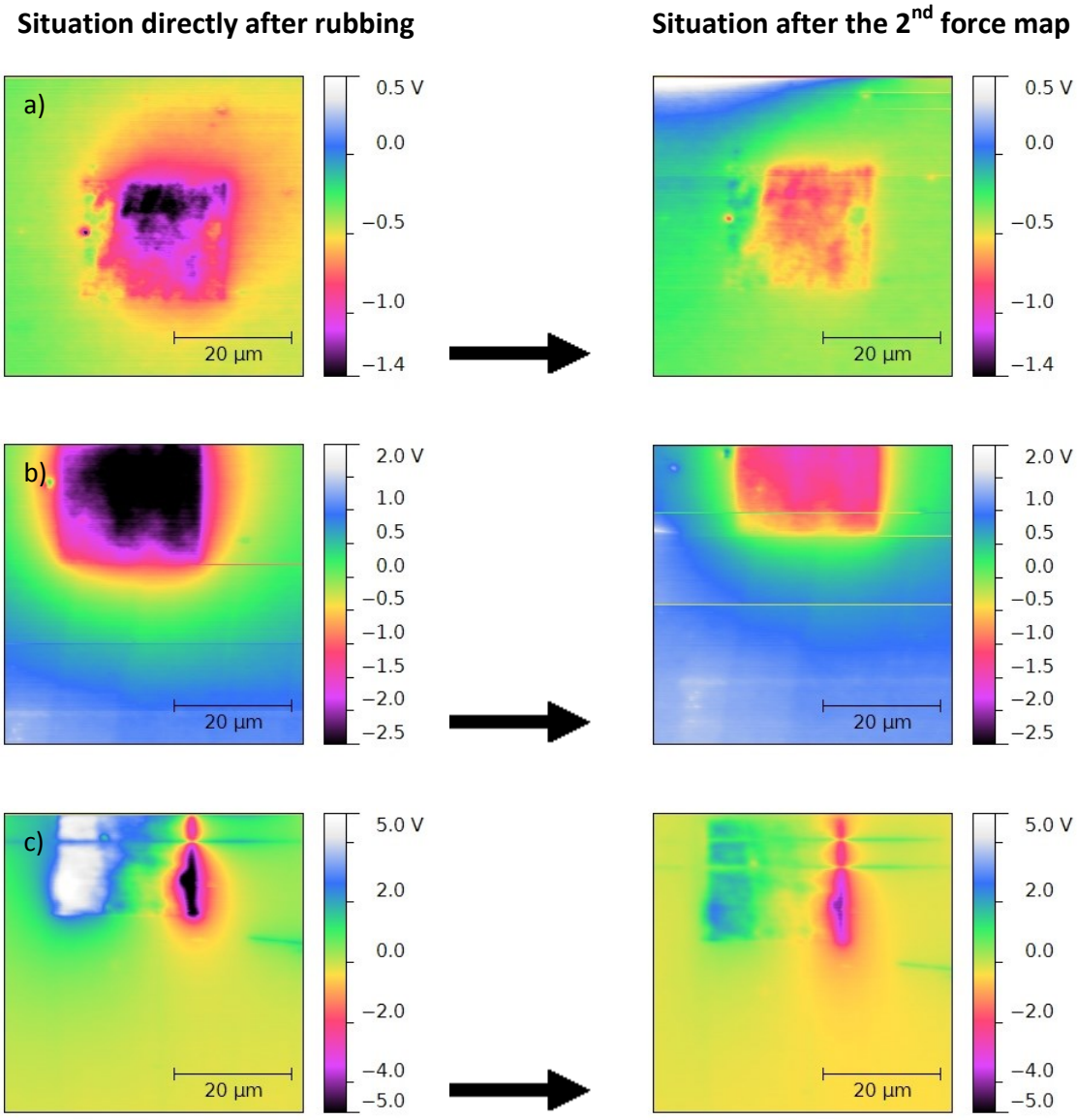

Figure 5.23: Decreasing of the CPD over time of different measurements. The left column presents the situation directly after rubbing. The right column is the situation after the 2nd force map. a) rubbing with calcite at 0.01 µN and 40 °C; b) rubbing with calcite at 0.1 µN and 40 °C; c) rubbing with quartz at 0.1 µN and 40 °C.

The time dependent change of surface charge can be worked out with so called long term measurements.

5.5 Long term measurements

In the long term measurements, the used measurement sequence was the same to get equivalent results, but the number of recorded images after the second force map was increased. Within the former process, only one single KPFM image was recorded after the second force map step. Here, a sequence of 14 images every 1.25 h was recorded. For example the initial change in CPD between Figure 5.24a) and Figure 5.24b) is much larger than the change after some hours as visible by comparing Figure 5.24m) and Figure 5.24n). The additional KPFM images reveal that even 16 hours after rubbing the CPD is still not fully recovered. Apparently, the introduced surface change is rather short. These long-term measurements were done at a temperature of 30 °C and with a force of 0.1 µN.

Calcite

The KPFM images of Figure 5.24 show a sequence of CPD images over time. Figure 5.24a is the CPD map measured directly after the second force map. This is the situation which has been presented always in the images d) of the previous KPFM measurements (chapter 5.1). The rubbing area is well visible in the central part of the image. The rubbed area exhibits a potential gradient in scan direction (from left to right and from top to bottom). The left rim has a potential of -0.4 to -0.7 V, the right rim -0.9 to -1.6 V. The potential of the surface before rubbing is also negative (-0.2 V). A single rubbed line shows a stronger contrast than the others. This line is 5 µm from the top rim of the rubbed area. The tendency is the same as for the rest, but the CPD is more negative. Apparently, also the surrounding area is influenced by the tribocharging process. Here, only the top, bottom, and right areas with respect to the rubbed area are influenced, not the left side.

Compared to image Figure 5.24a), the KPFM image of Figure 5.24b shows the observed change in CPD value. The highest charged parts show a stronger decrease than the others. A slightly charged surrounding is visible again.

The charge of the surrounding area is gone after measuring the third (Figure 5.24c after 3.75 h) image. After this time the CPD of the rubbed area changed to -0.9 V in the highest charged and -0.3 V in the lowest charged parts. An overview over all images exhibits, that the changing of the CPD slows down over time. Some measurement show a non-monotonous evolution of the CPD. Between Figure 5.24f and Figure 5.24g is a small jump in CPD (-0.25 to -0.4 V).

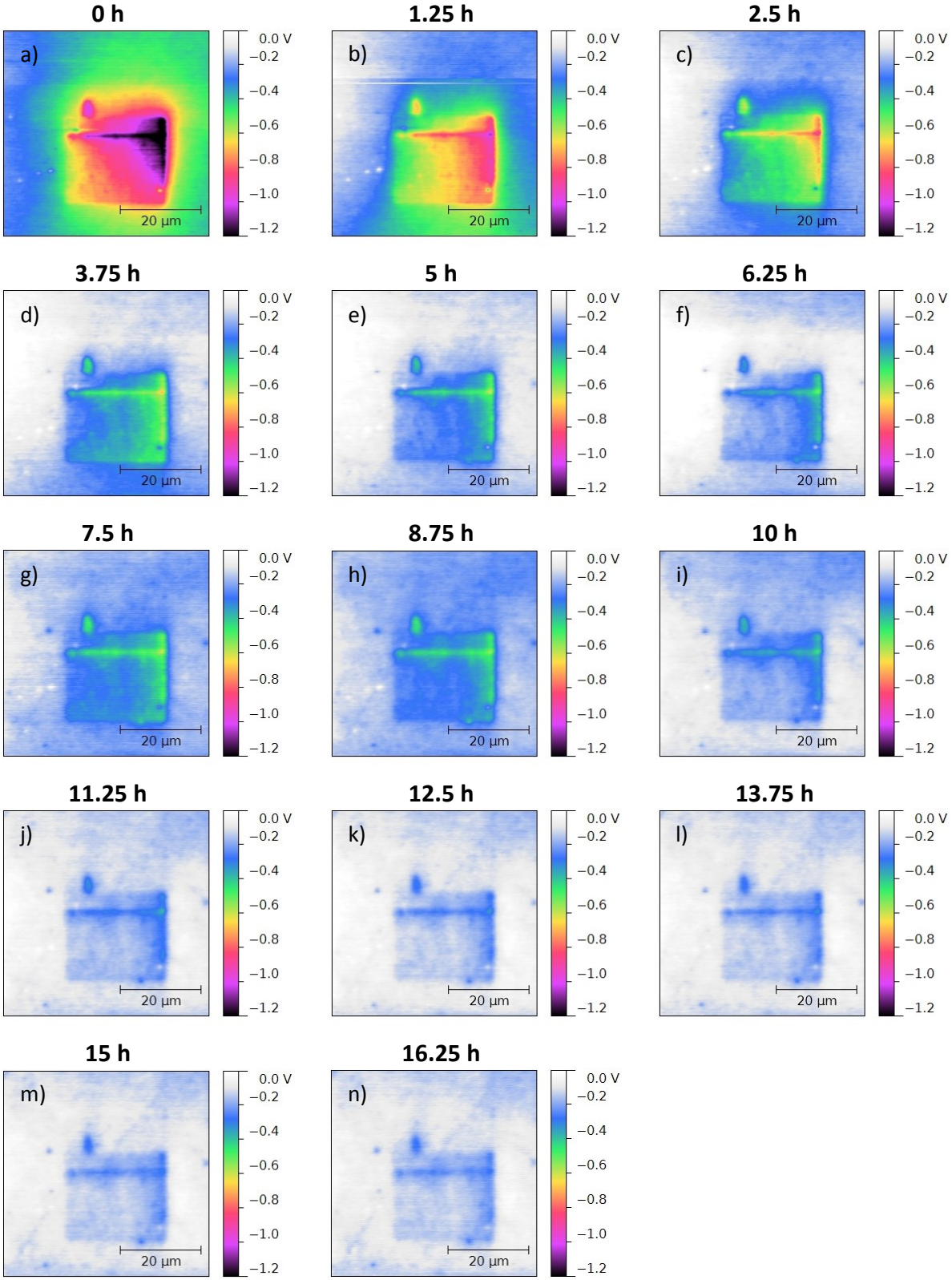

Figure 5.24: 50 x 50 µm^2 KPFM image of a calcite on $CaCO_3$(100) probe with a force of 0.1 µN and 30 °C. The KPFM images (a)-(n) present the situation after rubbing an area of 20 x 20 µm^2 with a time lag of 1.25 hours between image to image.

For a better analysis the CPD values are plotted as a function of time. This is presented in Figure 5.25. The blue line shows the average CPD of the investigated area, the red line is a simple exponential fit based on the formula a) $\mathrm{CPD} = \mathrm{y_0} + \mathrm{A} * \mathrm{e}^{\mathrm{R_0 * t}}$, b) $\mathrm{CPD} = \mathrm{A1} * \mathrm{e}^{-\frac{\mathrm{x}}{\mathrm{t1}}} + \mathrm{A2} * \mathrm{e}^{-\frac{\mathrm{x}}{\mathrm{t2}}} + \mathrm{y_0}$. The first exponential curve in Figure 5.25a) fits well to the measured CPD between 5 h and 16.25 h. The second exponential curve (Figure 5.25b), fits the measured signal better for shorter times (0 h to 5 h), than the first exponential fit. The small jump in CPD between 8 to 10 hours is better visible in the plot than in the KPFM images in Figure 5.24. This jump accounts for the CPD change between the images Figure 5.24f to Figure 5.24g. This offset is likely to be an artefact due to a temporal tip potential change.

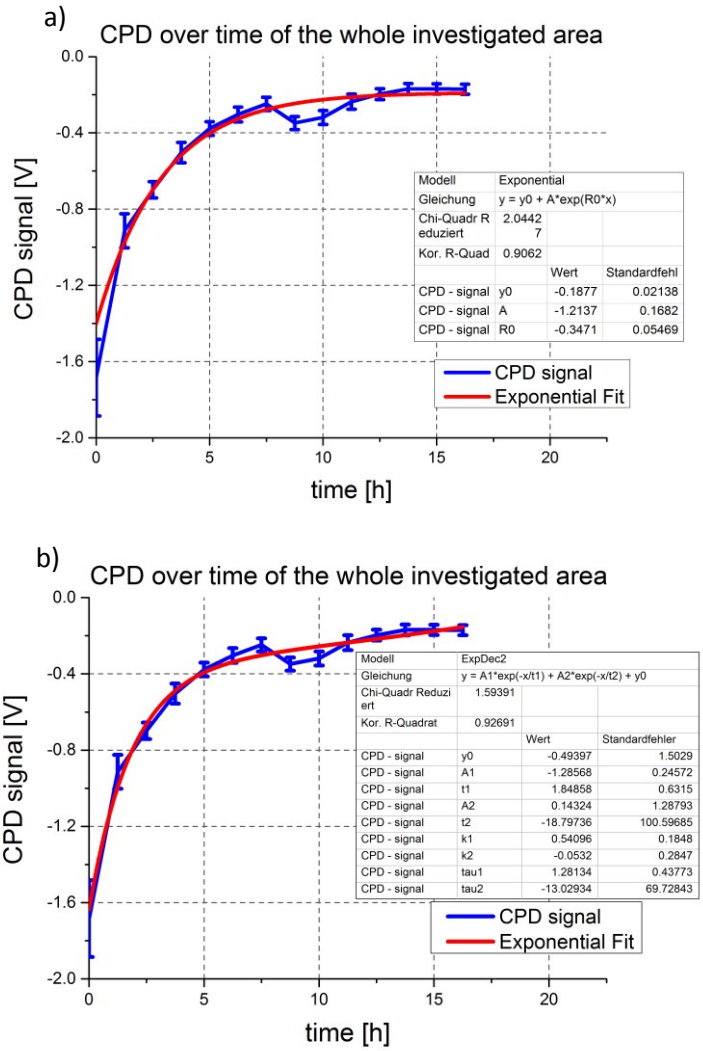

Figure 5.25: Average CPD value as a function of time by rubbing with a calcite particle at 0.1 µN and 30 °C. The decrease follows an exponential function:

a) $CPD = y_0 + A * e^{R_0 * t}$, b) $CPD = A1 * e^{-\frac{x}{t1}} + A2 * e^{-\frac{x}{t2}} + y_0$.

Quartz

Rubbing with quartz increases the CPD in contrast to rubbing with calcite which decreases the CPD. For comparison also long term measurements were done with the quartz rubbed surfaces. The time dependent evolution of the CPD is presented in Figure 5.26.

Image Figure 5.26a shows an almost homogeneous background surface, with a slight CPD value variation of 0 V to 0.5 V from top to bottom. Interestingly, the left and the right rim of the rubbed area exhibit negative CPD values (down to -1 V) whereas the central parts have positive CPD values up to 0.5 V. Both negative rims seem to have an influence on the CPD of the surrounding area in the lower parts in scan direction, whereas the positive central part not seems to be less influential.

The centre part shows no change with time, the surface potential of 0 V to 0.5 V Figure 5.26a stays constant even after 16.25 hours in (Figure 5.26m). The negatively charged rims, however, present a step by step increase of the surface potential over the time from -1 V to -0.3 V. The potential change slows down over time from image to image. This has also been seen on other measurements and confirms the results of other long-term measurement with the calcite particle.

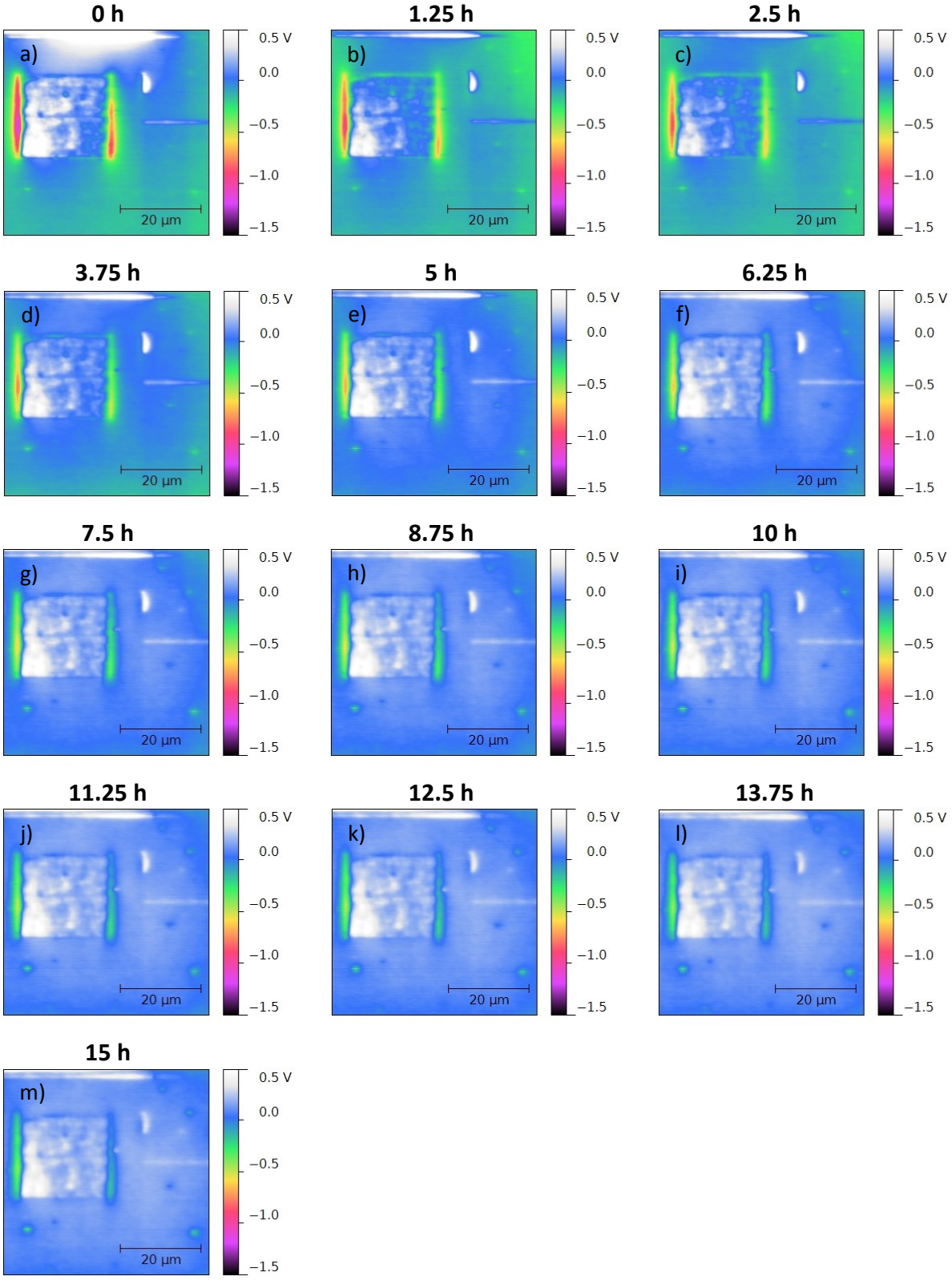

Figure 5.26: 50 x 50 µm^2 KPFM image of $CaCO_3$(100) rubbed by calcite with a force of 0.1 µN at 30 °C. (a)-(m) show KPFM images after rubbing an area of 20 x 20 µm^2 with a time lag of 1.25 hours from image to image.

The long term measurement after rubbing with quartz reveal some differences compared to the rubbing with the calcite particle. The results are plotted in Figure 5.27. The non-monotonic behaviour in the first 3 h might be caused by the two negatively charged areas on the left and right rim (in Figure 5.26). Every single measurement point of the KPFM represents the weighted average potential of the near surrounding area. This is schematically indicated in Figure 5.28. These influences might cause deviations from usually observed exponential behaviour.

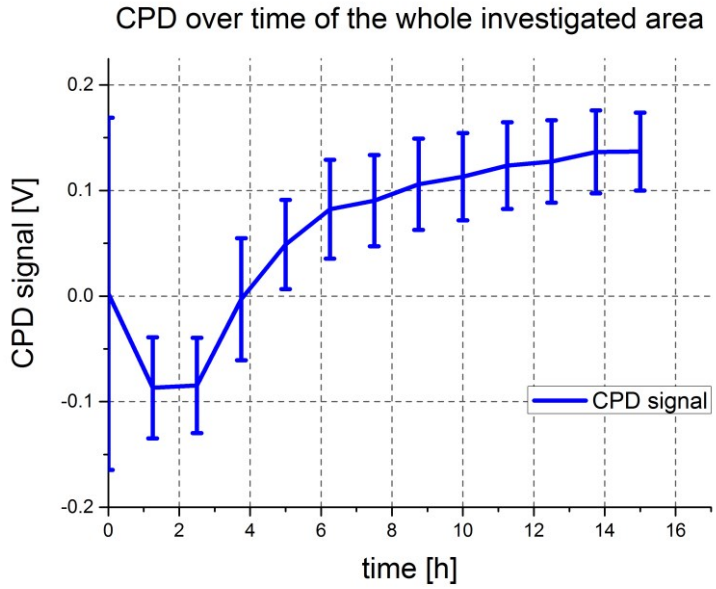

Figure 5.27: Average CPD value as a function of time of the long term measurement by rubbing with a quartz particle.

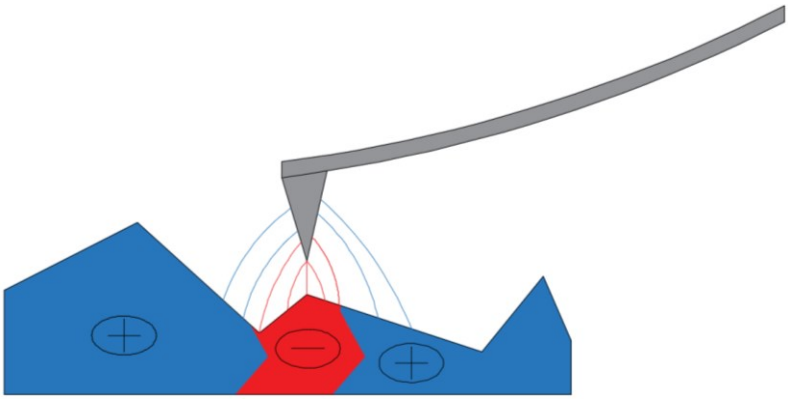

Figure 5.28: Influence of different surface charges on the KPFM measurement.

5.6 Force Distance Curve on the real system

FD curves can be used as a second analysing method. The higher the surface potential the higher the attractive forces on the cantilever. The cantilever starts a few µm above the surface. During the approach the attractive forces act on the cantilever, and bend it towards the surface. This bending can be analysed and the forces can be calculated. The two force map steps during the measurement sequence give a set of 32 x 32 FD curves before and after the rubbing with the mineral particle.

There are differences of the cantilever bending between the test system with the metal plate (chapter 4) in comparison to the real system with the 20 x 20 μm^2 rubbed area.

The test system uses a metal plate as surface material with an applied voltage to simulate the surface charging. The whole metal plate is charged, there is a large charged area under the cantilever (much larger than the cantilever dimension) to build a capacitor with the cantilever. The higher the potential difference, the stronger the bending of the cantilever towards the surface.

Figure 5.29 presents three examples for the cantilever bending at different applied voltages. The blue cantilever stands for 0 V, the green one for the maximum of 20 V and the red one in the middle for 10 V.

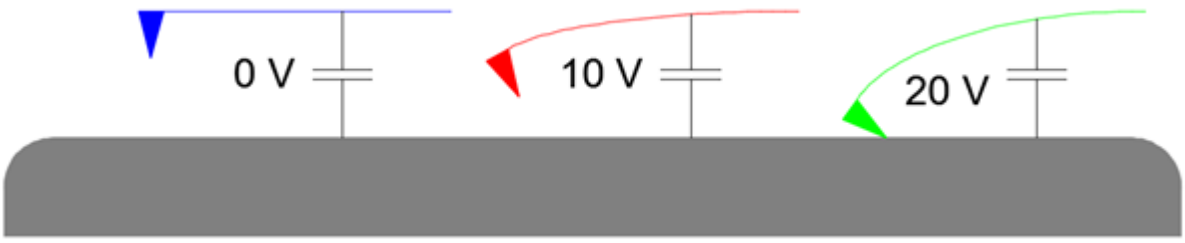

Figure 5.29: Three different bending of the cantilever, because of different applied voltages in the test system.

The real system, however, works a bit different to the test system. Differences are the size of the charged area and following the size of the conductor which is built between the surface and the cantilever. Figure 5.30 present the charged areas with a small yellow line on the sample surface under the tip. These charged areas have in reality a dimension of 20 x 20 μm^2, which corresponds to the size of the area, rubbed with the modified tip. Apparently, in the real measurements the capacitor is much smaller. Here, it is only built between the tip and the charged area. The lowest measured potentials are -9 V (rubbed with

calcite at 0.1 µN and 30 °C), so the effect of the smaller capacitor on the cantilever bending is much smaller compared to the test system.

Figure 5.30: Different bending of the cantilever,
because of different charging of the surface in the real system.

Figure 5.31 shows the measured FD curves of a real system in comparison to the test system. In this case (Figure 5.31), the FD curves were measured on $CaCO_3$(100) rubbed by calcite at 0.1 µN and 30 °C. Furthermore, this is the measurement with the lowest negative charge (-9 V) after the rubbing process. It has also the highest CPD difference between the rubbed area and the surrounding potential, in this case in total 7 V.

The surface positions of the presented blue and red FD curves are marked in the KPFM image in Figure 5.32 with a blue and red star. The black curve of the real system stands for the situation before the surface contact charging is performed, the position is equal to the red FD curve after the rubbing sequence. The diagram of Figure 5.31c is for comparison, it shows FD curves of the ideal test system with 0 V (black curve) and with 4 V (red curve). This comparison reveals the differences in attraction forces between a tip and surface with 7 V and the whole cantilever and surface with 4 V. The effect of the cantilever bending on the real system is much lower.

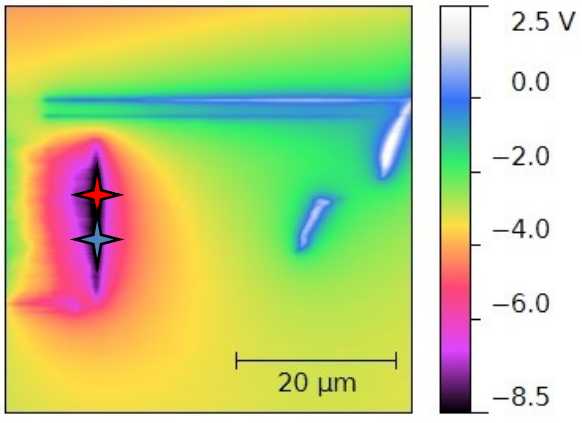

Figure 5.31: 50 x 50 µm^2 KPFM image of the 30 °C, 0.1 µN calcite sample. The red and blue stars define the position of the measured FD curves for comparison with the test system.

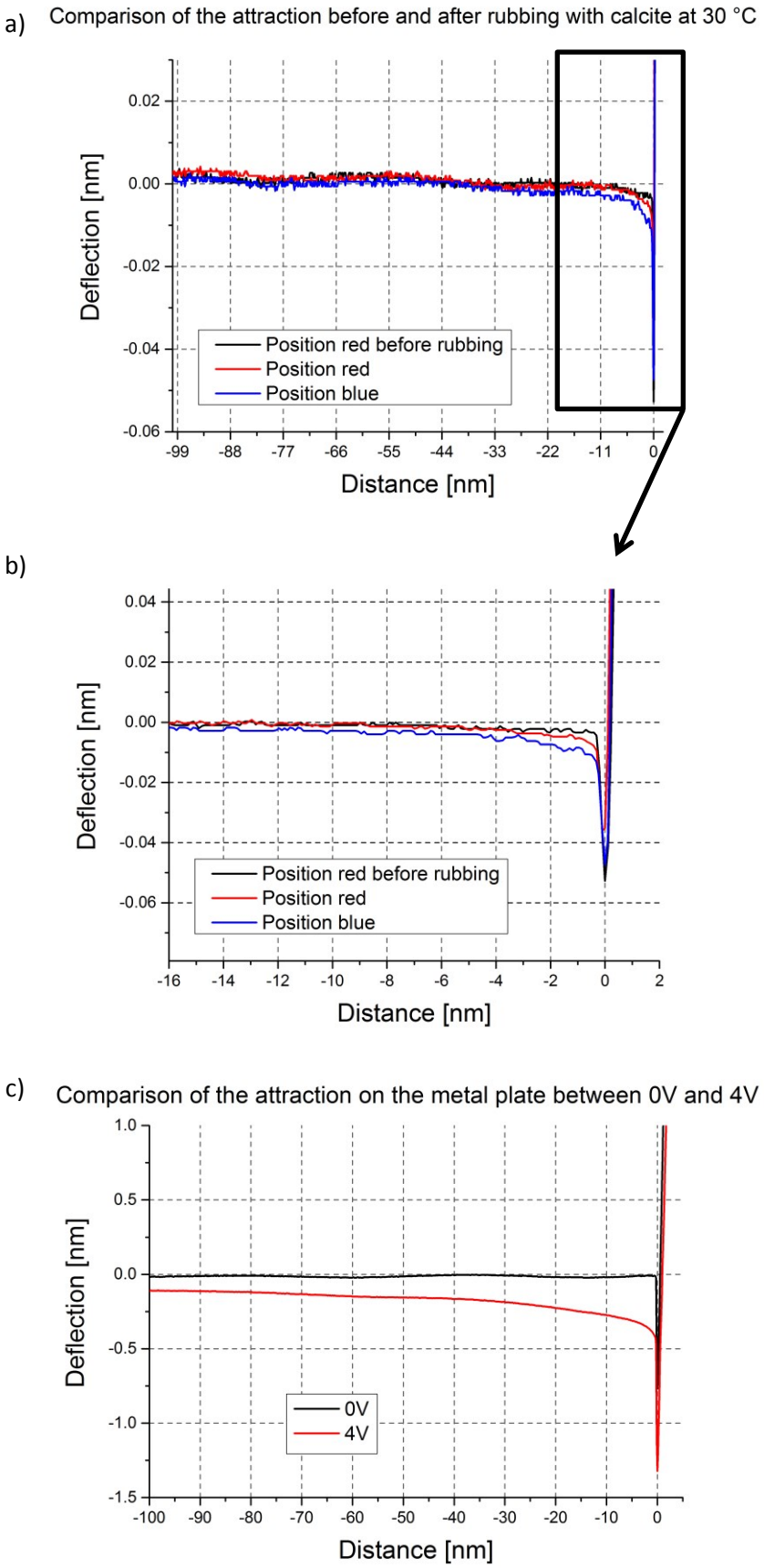

Figure 5.32: Comparison between the FD curves of the real system a) rubbing with calcite at 0.1 µN and 30 °C; b) zoomed FD curve; c) FD curves of the test system with the metal plate.

Figure 5.33 presents a second analysable result (rubbing with quartz 40 °C and 0.01 µN), which exhibit the bending of the cantilever. The red star marked the place of the two shown force distance measurements, before rubbing (black) and after rubbing (red). The CPD difference between the initial surface and the lowest charged parts of the rubbed area are 5 V. The attractive forces, in a distance of 10 nm, are strong enough that the cantilever jump into contact. There is no bending visible before it jump into contact.

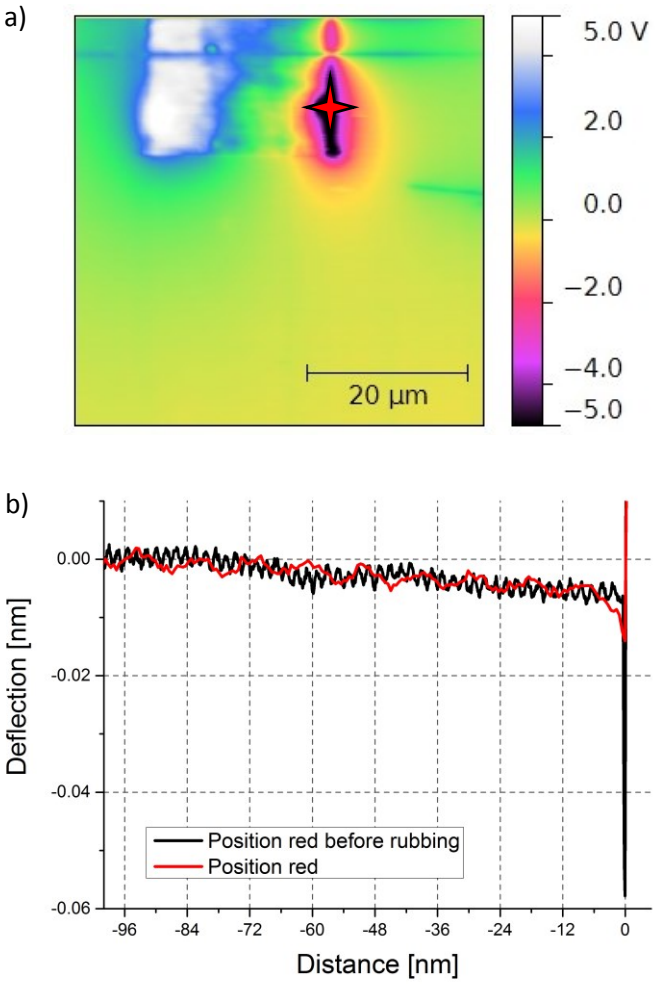

Figure 5.33: FD curve of the 40 °C, 0.1 µN quartz measurement on the same position (red star), before (black) and after (red).

5.7 Determination of the attraction force

In an AFM force distance measurement the electrostatic forces acting on the AFM probe are transduced in a cantilever deflection, which is measured via the reflection of a laser beam from the back side of the cantilever [31]. Knowing the mechanical properties of the cantilever (Table 5.1) allows the calculation of the actual force.

However, even though the force map of the test measurements and the rubbing experiments are based on the same cantilever type (NSG30/TiN), but a direct comparison is not possible. The reason for this is a difference in the loading mode. For the test measurement a voltage was applied to the cantilever (to simulate charge) causing a capacitive force acting as a distributed load all along the probe. In contrast, in the rubbing experiments the force is acting primarily on the tip, representing a point load.

A one sided clamped beam can act as model system for an AFM cantilever. The real system with the small charged area under the tip is like a beam with a single force at the end ($w_{(l)} = w_{max} = \frac{Fl^3}{3EI}$). The model system with the metal plate stands for a beam with distributed load ($w_{(l)} = w_{max} = \frac{ql^4}{8EI}$) [23] (see Figure 5.34a and Figure 5.34b).

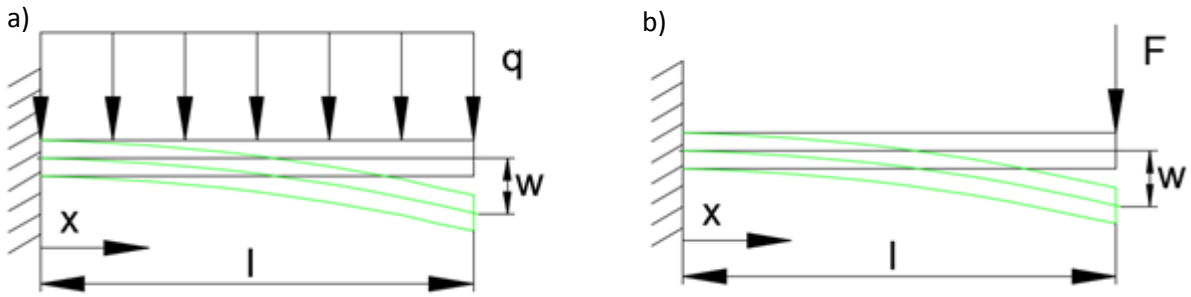

Figure 5.34: Model for the different loading modes:
a) beam with distribution load; b) beam with single load on the free end.

Table 5.1: Properties of the AFM probe NSG30/TiN [10].

Cantilever length, L ± 5 µm	Cantilever width, W ± 5 µm	Cantilever thickness	Force constant	Mass density
l	b	h	c	ρ
125 µm	40 µm	4 µm	22–100 N/m	2336 kg/m^3

For the measurements a typical mean force constant of 40 N/m was chosen [10]. The first calculations like the cross section or the young's modulus were used for both loading modes. These are independent of the loading mode, and can be calculated from the cantilever geometry (Table 5.2).

Table 5.2: Raw data which are used for the force calculations for both loading modes.

Cross section	Young's modulus	Mass of the cantilever	Torque of inertia
$\boldsymbol{A = b * h}$	$\boldsymbol{E = \frac{c * l}{A}}$	$\boldsymbol{m = A * l * \rho}$	$\boldsymbol{J = \frac{1}{12} * m * (h^2 + b^2)}$
$1.6 * 10^{-6}\ m^2$	$31250000\ {}^{N}/_{m^2}$	$4.672 * 10^{-11}\ kg$	$6.292\ kg\ m^2$

The rubbing with a calcite particle with 0.1 µN at 30 °C exhibits a maximum CPD difference of 7 V compared to the pristine surface. In comparison, the measurement with quartz with 0.1 µN at 40 °C exhibits a maximum CPD difference of just 5 V between pristine and rubbed surface. In Table 5.3 and Table 5.4 the corresponding deflection values and the calculated forces are listed.

Table 5.3: Force calculation of the single force mode (rubbing with calcite 30 °C 0.1 µN).

Bending of the cantilever	Force
$\boldsymbol{w}$	$\boldsymbol{F = \frac{3 * w * E * J}{l^3}}$
$1.5 * 10^{-10}$ m	$4.53 * 10^{-11}\ N$

Table 5.4: Force calculation of the single force mode (rubbing with calcite 40 °C 0.1 µN).

Bending of the cantilever	Force
$\boldsymbol{w}$	$\boldsymbol{F = \frac{3 * w * E * J}{l^3}}$
$1 * 10^{-10}$ m	$3.02 * 10^{-11}\ N$

It was expected that the force for this single calcite rubbed sample is higher than for this presented quartz sample, because of the larger CPD change for calcite.

The CPD difference between pristine and rubbed area of the calcite sample is 1.4 times (7 to 5 V) higher than on the quartz sample. Also the calculated forces ($4.53 * 10^{-11}\ N$ to $3.02 * 10^{-11}\ N$) result in a 1.5 times higher value on the calcite sample.

For comparison the loads of the test system are also calculated. The results of the 4 V, 8 V and 20 V measurements are presented in Table 5.5, Table 5.6, and Table 5.7. The first two (4 V and 8 V) are most comparable to the real measurements, because the rubbing leads to a similar CPD difference between cantilever and surface (7 V calcite and 5 V quartz). The third calculated force corresponds the measurement with 20 V, at is the maximum force, which can be achieved with the used test procedure.

Table 5.5: Force calculation of the distribution mode (metal plate 4 V).

Bending of the cantilever	Distribution force	Force on full cantilever length
$\boldsymbol{w}$	$\boldsymbol{q = \frac{8 * w * E * J}{l^4}}$	$\boldsymbol{F_{cant} = \frac{q}{l}}$
$0{,}5 * 10^{-9}$ m	$3.22 * 10^{-6}\,{}^{N}/_{m}$	$4.02 * 10^{-10} N$

Table 5.6: Force calculation of the distribution mode (metal plate 8 V).

Bending of the cantilever	Distribution force	Force on full cantilever length
$\boldsymbol{w}$	$\boldsymbol{q = \frac{8 * w * E * J}{l^4}}$	$\boldsymbol{F_{cant} = \frac{q}{l}}$
$1 * 10^{-9}$ m	$6.44 * 10^{-6}\,{}^{N}/_{m}$	$8.05 * 10^{-10} N$

Table 5.7: Beam with a distribution load mode (metal plate with maximum at 20 V.

Bending of the cantilever	Distribution force	Force on full cantilever length
$\boldsymbol{w}$	$\boldsymbol{q = \frac{8 * w * E * J}{l^4}}$	$\boldsymbol{F_{cant} = \frac{q}{l}}$
$6 * 10^{-9}$ m	$3.87 * 10^{-5}\,{}^{N}/_{m}$	$4.83 * 10^{-9} N$

All calculated forces are summarised in Table 5.8.

Table 5.8: Summary of all calculated forces.

Load mode	Sample	Bending	Force [N]
Single	rubbing with calcite 30 °C 0.1 µN	$1.5 * 10^{-10}$ m	$4.53 * 10^{-11}$
Single	rubbing with calcite 40 °C 0.1 µN	$1 * 10^{-10}$ m	$3.02 * 10^{-11}$
Distribution	Metal plate 4 V	$3.22 * 10^{-6}\,{}^{N}/_{m}$	$4.02 * 10^{-10}$
Distribution	Metal plate 8 V	$6.44 * 10^{-6}\,{}^{N}/_{m}$	$8.05 * 10^{-10}$
Distribution	Metal plate 20 V	$3.87 * 10^{-5}\,{}^{N}/_{m}$	$4.83 * 10^{-9}$

The test system is subject to a different loading mode, with a larger charged area under the cantilever. This makes it hard to compare the results with the real measurements. Therefore, the forces of the test system, are one to two orders of magnitude higher than on the real measurements.

5.8 Difference in charging between calcite and quartz

Rubbing with a mineral particle on a $CaCO_3$(100) surface leads to a potential change of the surface. In this thesis, the influence of two different minerals on contact electrification of the $CaCO_3$(100) surface has been investigated. Figure 5.35, summarizes these changes in surface potential due to rubbing with calcite (a) and quartz (b).

Rubbing with a calcite particle on a $CaCO_3$(100) surface (Figure 5.35a) results in a negative surface potential. For most experiments a similar change in surface potential of 0.5 to 1 V is observed. The only exception is the measurement with 0.1 µN and 40 °C. Here, the initial surface has a surface potential of +1.5 V, the rubbed area -2.2 V.

In contrast, rubbing with a quartz particle has an opposite influence on the surface potential. Here, the rubbing results in a positive surface potential. The range of the surface potential charge is again between 0.5 to 1 V.

Interestingly for both cases no systematic influence of the initial surface conditions (initial CPD) on the charging result has been found. This indicates that within the applied parameters the surface charging seems to be independent of the initial charge state of the surface.

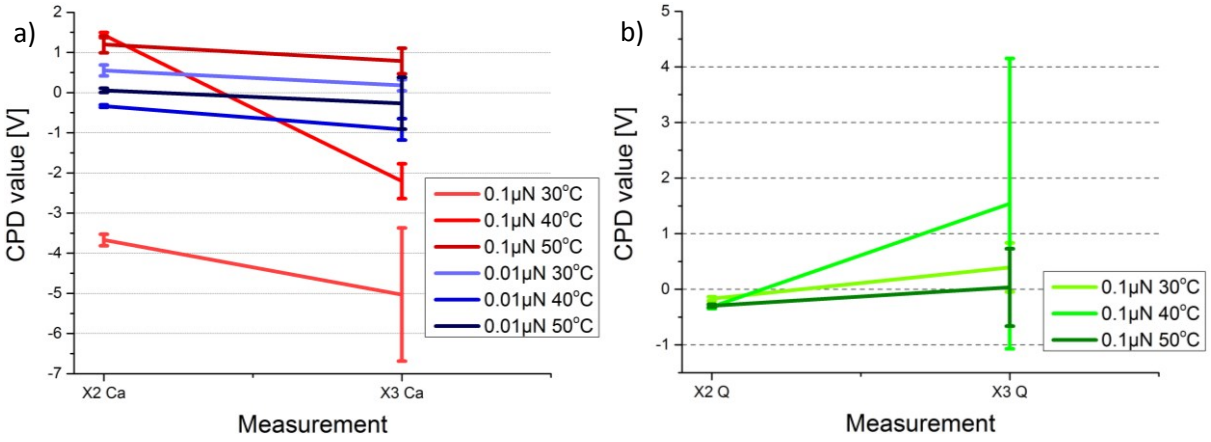

Figure 5.35: Comparison of the CPD value before (X2) and after (X3) rubbing by: a) calcite on $CaCO_3$(100) with 2 different forces (0.01 µN and 0.1 µN); b) quartz on $CaCO_3$(100) with 0.1 µN.

5.9 Influence of the force map on the surface

Rubbing with a mineral particle, changes the CPD of the investigated area. Decreasing CPD values are obtained for calcite particles, and increasing values for quartz particles. The CPD of the rubbed area, has the tendency to change back to the surface potential of pristine surface over time.

Within the measurement sequence, are two additional analysing steps which involve rather strong interaction with the surface beside the rubbing with the modified tips. These are the two force mapping steps between the two KPFM measurements before and after rubbing. One force map sequence consists of many single force distance curves (here 32 x 32). For each force distance curve, the tip touches the surface for a certain time (significantly longer and harder as the contact during tapping mode). So, there are 1024 touching points at which the probe interacts with the surface. Because of the small distance (1.56 µm from point to point, see Figure 5.36) the local charge in CPD are hard to resolve but rather merge to an overall change in CPD. The single points are only visible in one single KPFM measurement of the sample rubbed with the calcite particle with 0.1 µN at 50 °C. There the individual touching points are well visible (Figure 5.36). From this one can see the strong contribution of the center to the CPD (high density of touching points) and the weaker contribution of the rims (low density of touching points).

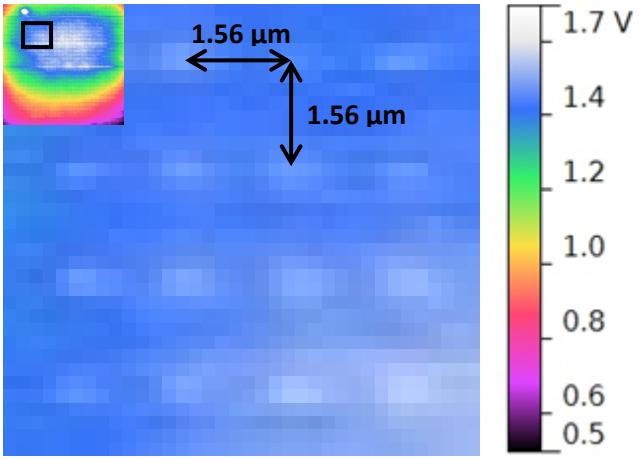

Figure 5.36: Distance between two FD curves in during the force map sequence.

On all other experiments the single contact points are not visible in the KPFM images, but there is nevertheless an influence of the force map on the CPD. This influence of the different force map sequences on the $CaCO_3$(100) surface are presented in Figure 5.37,

Figure 5.38, and Figure 5.39. The presented situations are between the KPFM measurements before and after rubbing.

The sample surface ($CaCO_3$(100)) and the measurement system (AFM) are the same for all data should be well comparable.

The CPD values before and after force mapping on calcite (at 0.01 µN) presented in Figure 5.37 reveals changes in the CPD due to force mapping, but do not show a systematic trend. The only systematic change is due to the rubbing, which leads to a decrease of the CPD (between the situations X2 and X3).

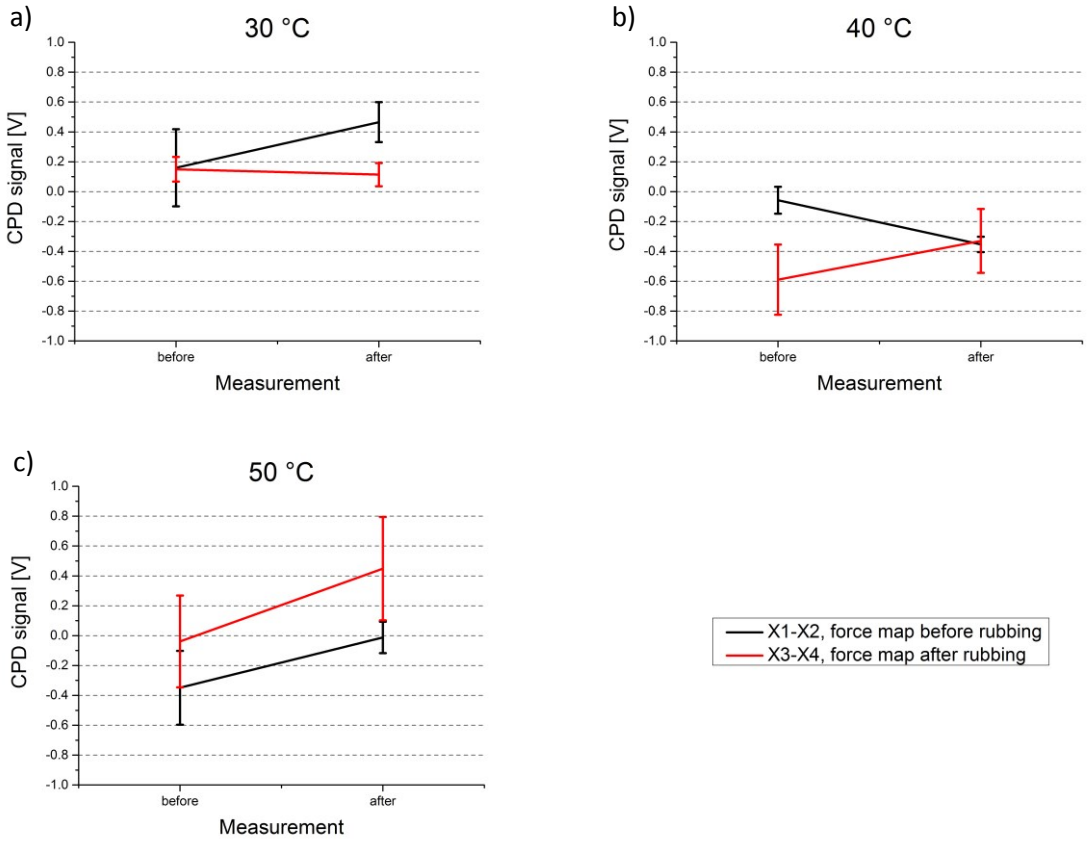

Figure 5.37: Influence of the force map on the $CaCO_3$(100) surface potential (experiment: rubbing with calcite at 0.01 µN) and a) 30 °C, b) 40 °C, and c) 50 °C. X1-X2 is the situation between the two KPFM measurements before rubbing, and X3-X4 the situation between the KPFM after rubbing.

Nearly all force maps executed within the experiments for calcite rubbed with 0.1 µN, increased the CPD of the surface. Only the force map X3-X4 of the experiment at 50 °C exhibits a small decrease. Figure 5.38 presents also the decrease of the surface potential by comparing the situations X2 with X3. The potential of the X3 situations (after rubbing) is lower than X2 (before rubbing). This is good visible in Figure 5.38, because here, the rubbing leads to a nice square shaped rubbed area with a strong change in CPD in comparison to the

CPD of situation X2. It can also be asserted that, the larger/lower the CPD before the stronger the change after the force map. This is consistent with the evolution of the CPD over time which is usually observed.

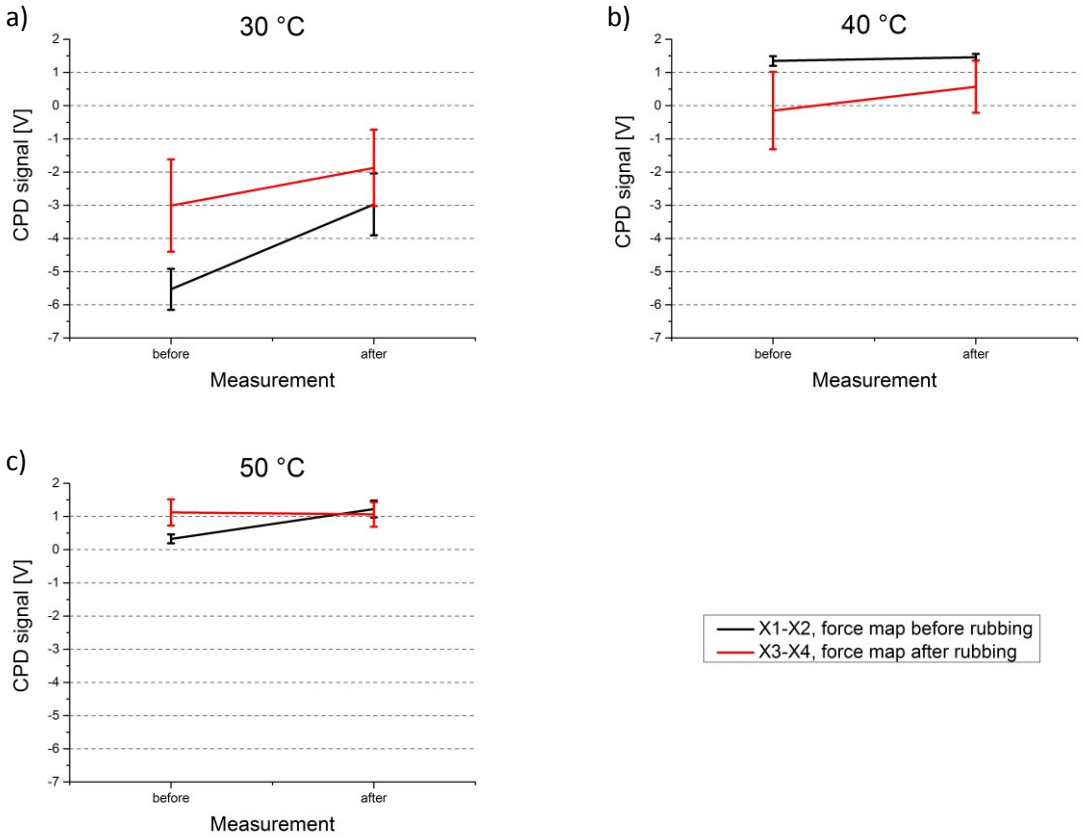

Figure 5.38: Influence of the force map on the $CaCO_3$(100) surface potential (0.1 µN rubbing with a calcite particle experiment) and a) 30 °C, b) 40 °C, and c) 50 °C. X1-X2 is the situation between the two KPFM measurements before rubbing and X3-X4 the situation after rubbing.

Here (Figure 5.38), all force maps (X1 to X2 as well as X3 to X4) of the measurements with the quartz particle tend to cause the CPD to go towards 0 V. All three cases show a small negative surface potential before the rubbing. The difference to the charging is also visible. The increase of CPD because of rubbing with the quartz particle (CPD of X2 is lower than the CPD of X3).

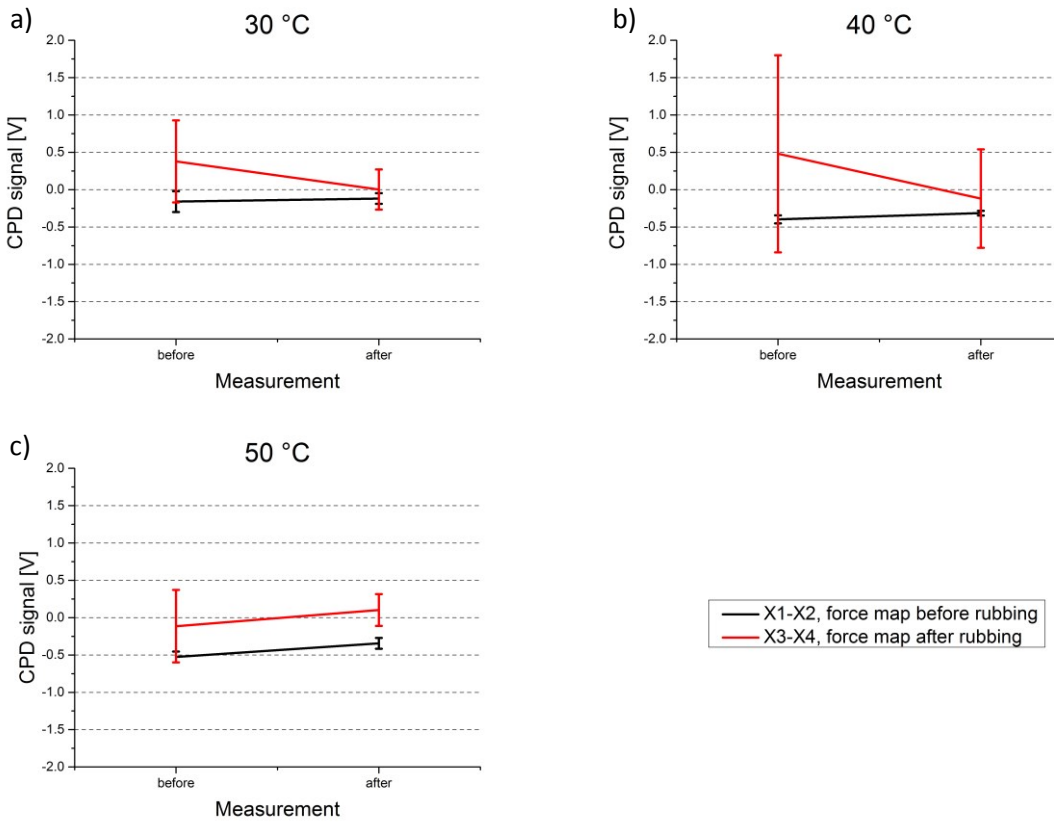

Figure 5.39: Influence of the force map on the $CaCO_3$(100) surface rubbed with a quartz particle at 0.1 µN and a) 30 °C, b) 40 °C, and c) 50 °C. X1-X2 is the situation between the two KPFM measurements before rubbing and X3-X4 the situation after rubbing.

5.10 Particle changes because of the rubbing process

All of the measurements were executed following the same sequence and for the same surface material ($CaCO_3$(100)). Parameters like the rubbing material (calcite or quartz), the force (0.1 µN and 0.01 µN) and the temperature (30 °C, 40 °C, and 50 °C) were varied. Figure 5.40 provides the six different surface potential situations of the rubbing experiments with calcite on $CaCO_3$(100). Interestingly the resulting CPD patterns on the charged 20 x 20 µm^2 area are quite diverse, ranging from homogeneous presented in Figure 5.40e to bipolar Figure 5.40c. The dimensions of all of them are roughly 20 x 20 µm^2, confirming that the mineral particle just touch the surface at a single point. For a multi-point contact, deviations of the 20 x 20 µm^2 square shape would be expected.

The surfaces are very flat with a root mean squared (rms) roughness of typically 5.5 nm (chapter 4.2). Therefore, the differences in the charge patterns are not a roughness effect. A stronger influence might be caused by the widely varying surface potential present before

the rubbing experiments. This might indicate an already present surface charge on the pristine surfaces.

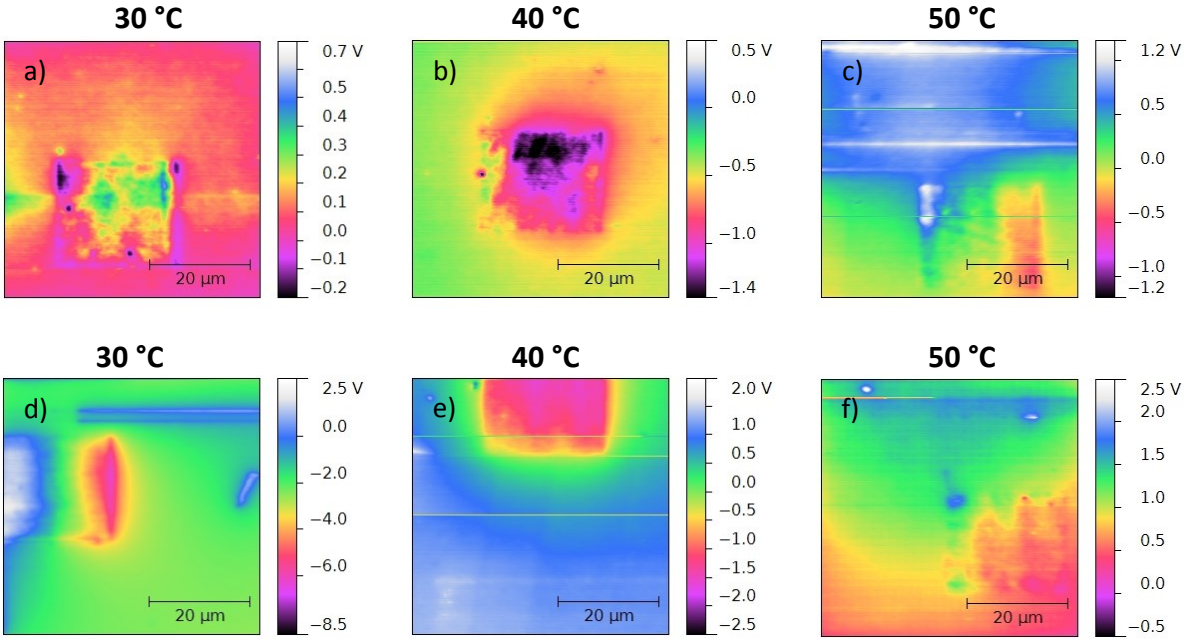

Figure 5.40: Different shapes of the measurements rubbing with calcite on $CaCO_3$: a)–c) 0.01 µN and d)–f) 0.1 µN.

Apparently, a further possible cause for the different CPD patterns is the change of the glued particle and not of the surface. The particle can change its shape due to the rubbing process. Therefore, comprehensive SEM images of the modified tips after use were performed. Figure 5.41 shows calcite modified probes before and after use. Image Figure 5.41a) presents the freshly prepared calcite particle, and image Figure 5.41b) the situation after all rubbing experiments were finished. Interestingly, there are no geometrical changes of the particle visible. Neither broken spikes nor rounded edges are detectable. Of course the particle itself in general will also charge up. However, at the moment it is not possible to access the particle charge.

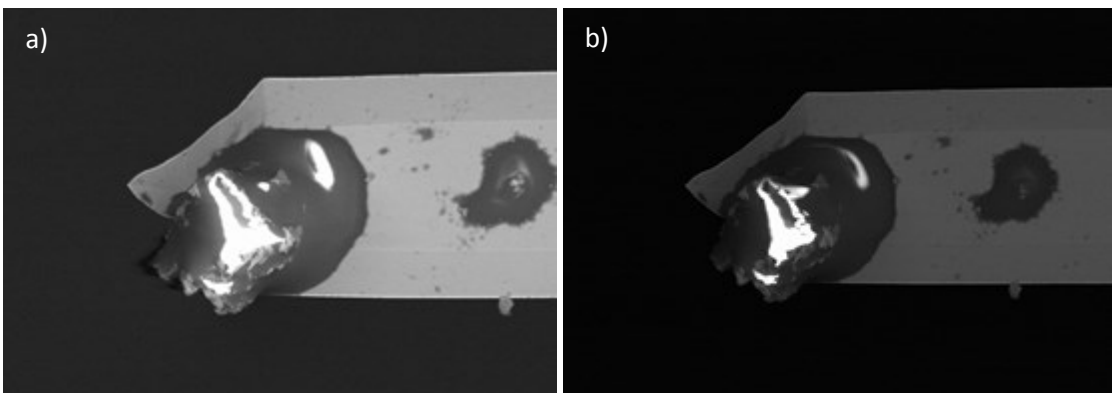

Figure 5.41: Shape of the attached calcite particle: a) before the first use and b) after usage.

For a better understanding of the contact between tip and surface, the real 3D geometry of the top of the particle has to be known. The only possibility to obtain this is with a tip characterizer (TGT 01 from NT – MDT) [7]. Figure 5.42 present the geometry of the only available test grating. There, the distance between two peaks is 2.12 µm and the height h is 0.3 µm to 0.5 µm. However, the size of the glued calcite particle is around 20 µm, thus it was not possible to get useful results using the available tip characterizer.

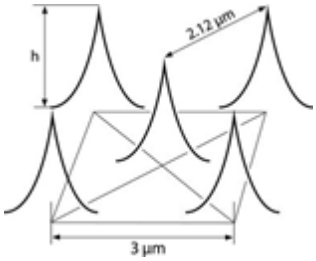

Figure 5.42: Geometry of the test grating TGT 01 from NT – MDT.

5.11 Influence of the temperature and diffusion

In the following chapter, the influence of the rubbing temperature on the results is discussed. In general, the higher the temperature, the higher the rate of diffusion. This holds also true for the diffusion of charge carrier. A body basically provides two possible modes of diffusion, these are surface and volume diffusion. Normally volume diffusion is larger, because of the higher diffusion cross section in comparison to surface diffusion [12]. The charge carriers in insulators is not clear which diffusion path dominates. Moreover charge carrier is influenced by electric fields causing additional directed drift motions.

This diffusion/drift is indirect visible on all measurements, because of the CPD change over time of the charged parts of the surface. There would be no change of CPD, if there would be no diffusion/drift. The two executed long term experiments give an idea how strong this effect is. They present an exponential change of the CPD over time. The effect is quite slow, because after 15 hours of measurement is still surface charge left. Indeed the exponential CPD decay indicates drift as the main cause of charge loss because a diffusion limited process should exhibit a square root dependence on time.

The normal measurements were done at three different temperatures. The temperature difference between 30 °C to 50 °C is apparently too low to cause a measurable difference in charging of the $CaCO_3$(100) surface. Also the image acquisition time (every 1.25 h) after the rubbing sequence is too long to resolve differences in the drift process. To make a clear statement on the diffusion/drift and the temperature effect on the change of the surface charge (CPD) over time more measurements are necessary.

6 Conclusion and Outlook

6.1 Conclusion

In this work, the triboelectric charging of $CaCO_3$(100) surfaces upon contact with a few 10 µm size mineral particles (calcite and quartz) has been investigated. The first requirements to perform such investigations systematically are to rub a µm size particle with defined force and speed against the surface. This requirement has been fulfilled by gluing single particles to the end of an AFM cantilever. In this way it is possible to use the highly sensitive AFM feedback to control and measure forces even below the nN regime. Further, the high lateral resolution AFM allows to perform rubbing experiments just on the µm-scale. Further, a monitoring of the built up surface change is necessary. An indirect method to visualise the surface change is to measure the surface potential. A measurement procedure with a defined sequence of AFM and KPFM measurements and surface manipulation steps was developed. Two different contact forces (0.1 µN and 0.01 µN) and three different temperatures (30 °C, 40 °C, and 50 °C) were used.

First, some test measurements were done to get an idea if the system will work. The rubbing was tested with a point, line and area charge. There was also the idea that the difference of the CPD – value before and after rubbing can be analysed with force distance curves. A higher surface potential leads to a higher attraction force and cantilever bending. The first test measurements on a system with a metal plate as substrate presents a good measureable influence of this surface potential changes. The problem in comparison to the real system is the size of the charged area under the cantilever. The test system forms a capacitor with the whole cantilever, the real system only with the tip. It is not possible to compare the height of cantilever bending between the real and the test system. With the experience of the preliminary tests a measurement sequence was developed. This contains four AFM height and KPFM measurements, one rubbing and two force map steps. The investigated area has a size of 50 x 50 μm^2 and the rubbing with the mineral particle 20 x 20 μm^2. Interestingly, the shape of the potential development is very different in the different measurements, although the surface is always the same. Some have a charging gradient in fast scan axis others have negative charged rims and a positive center. Only one single measurement (0.1 µN with 40 °C rubbing calcite particle on $CaCO_3$(100) surface) shows a homogeneous negatively charged rubbed area. The shape of the rubbed area

depends not on the particle, because all calcite measurements were done with the same cantilever. This was tested by analysing the shape of the glued mineral particle by SEM. This reveals, that the particle shows no difference before and after all measurements were done. The two different mineral materials show differences in the charging of the surface. Calcite decrease and quartz increase the CPD of the surface. Quartz shows a second difference in comparison to calcite. Quartz is much harder than calcite (Mohs hardness 7 quartz to 3 calcite). This hardness is the reason why surface wear is visible during every quartz measurement, which is usually observed in the measurements with calcite. The charging area indicates a changing of CPD over time. Two long term measurements (one with quartz and the other with calcite) were performed to analyse this effect. 15 images were done, one ever 1.25h getting measurable results. Both present the same results, the change of surface potential follows a simple exponential function ($\mathrm{CPD} = \mathrm{y_0} + \mathrm{A} * \mathrm{e}^{\mathrm{R_0 * t}}$ or $\mathrm{CPD} = \mathrm{A1} * \mathrm{e}^{-\frac{\mathrm{x}}{\mathrm{t1}}} + \mathrm{A2} * \mathrm{e}^{-\frac{\mathrm{x}}{\mathrm{t2}}} + \mathrm{y_0}$). All measurements exhibit an influence on the surrounding of the rubbed area. This influence is different around the positive and the negative charged parts. Apparently, there is also a difference in fast and slow scan axis.

6.2 Outlook

In this diploma thesis, the measurements were done under ambient conditions at 30 °C, 40 °C, and 50 °C. For a better understanding of the influence of the temperature on the rubbing process, the use of higher temperatures over a larger range is necessary. At higher temperatures, thermal activated processes are accelerated. The local discharging might be associated with the thermal activated hopping of charge carriers between surface trap states. In this case, the affective surface conductivity is temperature dependent and might be determined by measuring the time evolution of the CPD at different temperatures. Further measurements can also be performed using different surface materials. All previous charging experiments have been carried out on the same $CaCO_3$(100) surface. So far as rubbing materials calcite itself and quartz were used. Using a quartz substrate would complete the picture. The influence of a quartz particle on a calcite surface is now known. An interesting question is how the system reacts with a quartz surface and how the charge distribution will behave with time. Further investigations under better controlled conditions will also improve the measurement results. The problem for ambient condition is the change of humidity between the measurements. The measurements in this thesis were typically done between 42 %RH and 55 %RH. A water layer can form on the surface, or oxygen might react with the sample surface. Controlled conditions, like a nitrogen atmosphere, can help to avoid these problems.

Acknowledgments

I will thank several peoples for helping and supporting me in the course of this diploma thesis.

Ao.Univ. -Prof. Dipl. -Phys. Dr.rer.nat. Christian Teichert
for his kind and excellent supervision, for giving me the opportunity to work in the SPM Group and to write this thesis and the correction of it.

Dipl. -Ing. Dr.techn. Markus Kratzer
for teaching me AFM and KPFM, for his excellent supervision, the kind and patient support and correction of this work.

Mgr inz. Monika Mirkowska
for teaching me AFM and KPFM, the kind and patient support and correction of this work.

Univ.-Prof. Dipl.-Ing. Dr.mont. Helmut Flachberger
for helpful discussion and financial support.

Dr.mont. MSc. Kartik Pondicherry
for making the SEM measurements of the modified AFM probes.

Heide Kirchberger and Ulrike Zepic-Soller
for administrative support.

OMYA GmbH
for helpful discussion and financial support.

Christian Ganser, Katharina Czibula, Patrice Kreiml, Jakob Genser, Michael Lassnik
for giving me a nice and fun time working in the SPM Group.

My Family
for sponsorship.

My Girlfriend
for helping me in all situations, help was needed.

My Grandma Purker and my Grandma Resi
for believing in me every time.

My Friends and Colleges
for a nice and fun time in Leoben.

References

[1] SADEWASSER, Sascha; GLATZEL, Thilo. *Kelvin probe force microscopy: measuring and compensating electrostatic forces*. Springer Science & Business Media, 2011.

[2] YANG, Gan. A review of techniques for attaching micro-and nanoparticles to a probe. s tip for surface force and near-field optical measurements. *Review of Scientific Instruments*, 78. Jg., S. 1-8, 2007.

[3] MIRKOWSKA, Monika, et al. Atomic Force Microscopy as a Tool to Explore Triboelectrostatic Phenomena in Mineral Processing. *Chemie Ingenieur Technik*, 2014, 86. Jg., Nr. 6, S. 857-864.

[4] BUTT, Hans-Jürgen; CAPPELLA, Brunero; KAPPL, Michael. Force measurements with the atomic force microscope: Technique, interpretation and applications. *Surface science reports*, 59. Jg., Nr. 1, S. 1-152, 2005.

[5] https://www.asylumresearch.com/Products/PolyHeater/PolyHeater.shtml, January 2015, Asylum Research.

[6] http://www.omya.com/calciumcarbonate-dolomite, January 2015, OMYA AG.

[7] http://www.ntmdt-tips.com/products/view/tgt1, January 2015, NT-MDT.

[8] C. Teichert. Rastersondentechniken zur Charakterisierung von Festkörperoberflächen. Vorlesungsskriptum an der Montanuniversität Leoben, 2009.

[9] P. Klapetek, D. Necas and C. Anderson. *Gwyddion user guide*, 2010.

[10] http://old.ntmdt-tips.com/catalog/golden/cond/non/tin/products/nsg30_tin_50.html, January 2015, NT-MDT.

[11] M. Panzenböck. Werkstoffprüfung. Vorlesungsskriptum an der Montanuniversität Leoben, 2011.

[12] BARGEL, Hans-Jürgen; SCHULZE, Günter (Hg.). *Werkstoffkunde*. Springer-Verlag, 2008.

[13] LOWELL, J.; ROSE-INNES, A. C. Contact electrification. *Advances in Physics*, 29. Jg., Nr. 6, S. 947-1023, 1980.

[14] BUNKER, Matthew J., et al. Direct observation of single particle electrostatic charging by atomic force microscopy. *Pharmaceutical research*, 24. Jg., Nr. 6, S. 1165-1169, 2007.

[15] MATSUSAKA, S., et al. Triboelectric charging of powders: A review. *Chemical Engineering Science*, 65. Jg., Nr. 22, S. 5781-5807, 2010.

[16] WIDENOR, Ross. *An Investigation of Contact Electrification and Triboelectric Charging in Insulating Materials.* Doktorarbeit. Case Western Reserve University. 2013.

[17] CAPPELLA, Brunero; DIETLER, Giovanni. Force-distance curves by atomic force microscopy. *Surface science reports*, 34. Jg., Nr. 1, S. 1-104, 1999.

[18] https://www.asylumresearch.com/Products/MFP-3DOrigin/MFP-3D_Origin_Brochure_HR.pdf, March 2015, Asylum Research.

[19] http://www.novascan.com/products/Halcyonics_micro40.pdf, March 2015, Accurion GmbH.

[20] BINNIG, Gerd; QUATE, Calvin F.; GERBER, Ch. Atomic force microscope. *Physical review letters*, 56. Jg., Nr. 9, S. 930, 1986.

[21] JANKOV, I. R.; GOLDMAN, I. D.; SZENTE, R. N. Principles of the Kelvin Probe Force Microscopy. *Revista Brasileira de Ensino de F ísica*, 22. Jg., Nr. 4, S. 503, 2000.

[22] MELITZ, Wilhelm, et al. Kelvin probe force microscopy and its application. *Surface Science Reports*, 66. Jg., Nr. 1, S. 1-27, 2011.

[23] RICHARD, Hans Albert; SANDER, Manuela. *Technische Mechanik: Festigkeitslehre*. Wiesbaden: Vieweg, 2006.

[24] https://www.norlandprod.com/literature/68tds.pdf, March 2015, Norland Products Inc.

[25] http://www.sibelco.be/Web/Sibelcobe/Site.nsf/lwebkey/Sibelco_TDS_01_Kwartsmeel_Sort001200-Millisil%20M6/$File/TDS_Millisil_M6_-_M10_(EN).PDF?Openelement, April 2015, Sibelco.

[26] http://www.mtixtl.com/CCO-a-101005-S1.aspx, April 2015, MIT Corporation.

[27] https://www.tedpella.com/AFM_html/AFM.htm#anchor842459, April 2015, Ted Pella Inc.

[28] Patent DE102005023950B: Anlage zur Herstellung disperser mineralischer Produkte. Angemeldet am 20.05.2005, veröffentlicht am 02.08.2007, Anmelder: OMYA GmbH, Gummern, AT, Erfinder: Mangelberger, Thomas, Dipl.-Ing., Villach, AT; Tavakkoli, Bahman, Dr., Puch, AT.

[29] BIRDI, K. S. *Scanning probe microscopes: applications in science and technology*. CRC press, 2004.

[30] http://www.zeiss.com/microscopy/en_de/products/scanning-electron-microscopes/evo-materials.html#introduction, April 2015, ZEISS.

[31] MEYER, Gerhard; AMER, Nabil M. Simultaneous measurement of lateral and normal forces with an optical-beam-deflection atomic force microscope. *Applied Physics Letters*, 57. Jg., Nr. 20, S. 2089-2091, 1990.

[32] KEMPE, Ulf, et al. Quartz regeneration and its use as a repository of genetic information. In: Quartz: *Deposits, Mineralogy and Analytics*. Springer Berlin Heidelberg, 2012. S. 331-355.

[33] LACKS, Daniel J.; SANKARAN, R. Mohan. Contact electrification of insulating materials. Journal of Physics D: *Applied Physics*, 44. Jg., Nr. 45, S. 453001, 2011.

[34] GREEN, Nicola H., et al. Force sensing and mapping by atomic force microscopy. *TrAC Trends in Analytical Chemistry*, 21. Jg., Nr. 1, S. 65-74, 2002.

[35] http://gwyddion.net/presentations/talk-roughness-David-Necas-2012.pdf, April 2015, Gwyddion.

[36] http://physik.unileoben.ac.at/de/1934/, April 2015, Montanuniversität Leoben.